





Original Article



Anti-photoaging Properties of Asiaticoside in Ultraviolet A-irradiated Human Dermal Fibroblasts by Activating the PI3K-AKT Pathway and Inhibiting the NF- κ B Pathway

Jia Huang^{1#}, Yiyi Gong^{1#}, Ke Liu^{2#}, Jun Chen^{2*}  and Xiaobo Zhou^{2*} 

¹Department of Dermatology, Huashan Hospital, Fudan University School of Medicine, Shanghai, China; ²Department of Dermatology, Shanghai Ninth People's Hospital, Shanghai Jiao Tong University School of Medicine, Shanghai, China

Received: May 24, 2023 | Revised: June 25, 2023 | Accepted: July 20, 2023 | Published online: August 16, 2023

Abstract

Background and objectives: Asiaticoside reduces inflammatory reactions and oxidative stress, the primary causes of photoaging. The authors speculated that asiaticoside might contain therapeutic potential for photoaging.

Methods: Network pharmacology and molecular docking were used to explore the mechanisms of asiaticoside in treating photoaging. After achieving the targets of asiaticoside using PharmMapper, SwissTargetPrediction, CTD and BATMAN databases, as well as, targets of photoaging using GeneCards database, the co-targets interaction network was formed and a network of asiaticoside, photoaging, and common targets were constructed by Cytoscape. Next, the common targets were analyzed using GO and KEGG enrichment.

Results: The analysis highlighted 202 core targets of asiaticoside were involved in the pathogenesis of photoaging. KEGG indicated asiaticoside performed an anti-photoaging effect through inflammation- and apoptosis-related signalling pathways, especially the PI3K-AKT and NF- κ B pathways. Furthermore, the anti-photoaging effect of asiaticoside was verified by human dermal fibroblasts with UVA irradiation *in vitro*.

Keywords: Asiaticoside; anti-photoaging; Anti-inflammation; Anti-apoptosis; Network pharmacology; Molecular docking.

Abbreviations: BATMAN, bioinformatics analysis tool for molecular mechanism of traditional Chinese medicine; BAX, BCL-2-associated X protein; BCL-2, b-cell lymphoma 2; BCL2L1, BCL2 like 1 (human); CCK-8, cell counting kit 8; CTD, comparative toxicogenomics database; ECM, extracellular matrix; GAPDH, glyceraldehyde 3-phosphate dehydrogenase; GO, gene ontology; HDFs, human dermal fibroblasts; I κ B α , nuclear factor of kappa light polypeptide gene enhancer in B-cells inhibitor, alpha; IL-6, interleukin 6; KEGG, Kyoto encyclopedia of genes and genomes; MAPKs, mitogen-activated protein kinases; MCC, Matthews correlation coefficient; MMP(s), matrix metalloproteinase(s); NF- κ B, nuclear factor kappa-light-chain-enhancer of activated B cells; p-AKT, phospho-AKT; P53, tumor protein p53; PI3K-AKT, phosphatidylinositol 3 kinase (PI3K)/protein kinase B (AKT); PIK3R1, phosphoinositide-3-kinase regulatory subunit 1; PPAR(s), peroxisome proliferator-activated receptor(s); PPAR γ , peroxisome proliferator-activated receptor gamma; PPI, protein-protein interactions; PTEN, phosphatase and tensin homolog; qPCR, quantitative polymerase chain reaction; ROS, reactive oxygen species; SMAD, suppressor of mothers against decapentaplegic; TGF β , transforming growth factor-beta; TIMP1, tissue inhibitor of the metalloproteinases 1; TNF- α , tumour necrosis factor- α ; UV, ultraviolet; UVA, ultraviolet A; VC, vitamin C.

*Correspondence to: Jun Chen, Department of Dermatology, Shanghai Ninth People's Hospital, Shanghai Jiao Tong University School of Medicine, 639 Zhizaoju Rd., Shanghai 200011, China. ORCID: <https://orcid.org/0000-0003-3633-6377>. E-mail: chenjun125125@126.com; Xiaobo Zhou, Department of Dermatology, Shanghai Ninth People's Hospital, Shanghai Jiao Tong University School of Medicine, 639 Zhizaoju Rd., Shanghai 200011, China. ORCID: <https://orcid.org/0000-0001-8827-2921>. Fax: 0086-21-6313-6856, E-mail: dr.zhouxb@foxmail.com

#These authors contributed equally to this work.

How to cite this article: Huang J, Gong Y, Liu K, Chen J, Zhou X. Anti-photoaging Properties of Asiaticoside in Ultraviolet A-irradiated Human Dermal Fibroblasts by Activating the PI3K-AKT Pathway and Inhibiting the NF- κ B Pathway. *Explor Res Hypothesis Med* 2023;8(4):319–337. doi: 10.14218/ERHM.2023.00037.

Conclusion: Asiaticoside may alleviate UVA-induced cell proliferation inhibition, reverse the abnormal gene expressions involved in the PI3K-AKT and NF- κ B pathways, and have a high affinity with those core targets.

Introduction

Skin is the first natural defense barrier that protects our body from exogenous stimuli. With skin aging caused by malnutrition, environmental pollutants, gravity, collagen loss, and ultraviolet (UV) irradiation, disrupted integrity of the skin barrier could be observed. Photoaging caused by UV irradiation (especially UVA) has been identified as the primary factor in skin aging, which results in skin roughness, reduced collagen content, decreased skin elasticity, deep wrinkles and pigment formation, causing cosmetic disability and psychological distress.^{1,2} UVA leads to skin photoaging by inducing the overproduction of reactive oxygen species (ROS), which could initiate intracellular oxidative stress, apoptosis, DNA damage, autophagy and cellular signalling events.² ROS could activate the NF- κ B signalling pathway via increasing phosphorylated (p-) I κ B α , causing an inflammatory “storm” by secre-

tion of multiple pro-inflammatory cytokines.³ Additionally, ROS also have a suppressed effect on the PI3K-AKT signalling pathway via lowering the expression of p-AKT, which could contribute to cell apoptosis.⁴ Excessive ROS accumulation and cell aging regulate longevity regulation pathway⁵ and stimulation of transforming growth factor β (TGF- β) signalling in UVA-irradiated human dermal fibroblasts (HDFs).⁶ Photoaged skin was characterised by the loss of dermal extracellular matrix (ECM) including various types of collagens by overexpressed matrix metalloproteinases (MMPs) and down-expressed tissue inhibitor of the metalloproteinases 1 (TIMP1).⁷ Moreover, enhanced signalling MAPK and NF- κ B, as well as, attenuated TGF- β /Smad and PI3K-AKT signalling could lead to decreased collagen and TIMP1 production under UVA irradiation.^{8,9} In addition, UVA irradiation could markedly down-regulate the mRNA expression of BCL-2 while upregulated BAX in HDFs,¹⁰ triggering the release of inflammatory factors like interleukin-1 beta (IL-1 β), interleukin 6 (IL-6), tumour necrosis factor- α (TNF- α) that eventually result in cell apoptosis and skin photodamage.¹¹ Therefore, the authors hypothesize that an anti-oxidant, anti-apoptotic, and anti-inflammatory agent could be an effective candidate to alleviate UVA-induced photoaging.

Currently, the trend is to use natural plant extracts with antioxidant and immunomodulation activity as safe and effective products to prevent or treat skin photoaging.^{12,13} Asiaticoside is a traditional Chinese herbal monomer extracted from *Centella Asiatica*, which has been used for many years to treat various skin diseases like skin ulcers, and scleroderma, to promote healing.^{14,15} *Centella Asiatica* has been reported to have a wide range of pharmacological effects that include anti-inflammation and anti-oxidation.^{16,17}

Chinese medicine is used to treat deficiencies in the body by strengthening the body, and has the advantages of multiple targets, as well as, minimal side effects compared to pharmaceutical treatments. Network pharmacology is a rapidly developing field that integrates computer science with clinical medicine, and researchers aim to analyze the molecular mechanisms of drugs by constructing, as well as, visualizing interaction networks involving multiple genes, targets, and pathways. Through this approach, network pharmacology can provide insights into the complex interactions between drugs and biological systems to help develop novel drug targets, as well as, treatment strategies.¹⁸ Molecular docking is a novel technique to identify the mechanism of drug binding to the molecular by network pharmacology.^{19,20}

The experimentation was initiated to clarify the mechanism of asiaticoside in preventing and treating UVA-induced skin photoaging through *in vitro* experiments with the help of network pharmacology.

Materials and methods

Identifying the targets of asiaticoside and photoaging

The targets of asiaticoside were retrieved from BATMAN, SwissTargetPrediction, PharmMapper, and comparative toxicogenomics database (CTD). A pioneer in providing an online bioinformatics tool to investigate molecular mechanisms of traditional Chinese medicine, the BATMAN-TCM database, is available at <http://bionet.ncpsb.org/batman-tcm>.²¹ The SwissTargetPrediction database (<http://www.swisstargetprediction.ch/>) predicts the targets of bioactive molecules by analyzing their chemistry.²² After importing line notations of asiaticoside into the BATMAN and SwissTargetPrediction database, information about targets was obtained. PharmMapper, which can be accessed at <http://lilab.ecust.edu.cn/pharmmapper/>, is an analytical tool capable of predicting a small molecule's biological targets by comparing it with all the experimentally determined three-dimensional protein structures available on PharmTargetDB.²³ After submitting the 3D structures and using default parameters, PharmMapper predicted the potential targets of asiaticoside. Meanwhile, CTD (<http://ctdbase.org/>) is a freely accessible database that offers curated information on chemical-gene/protein interactions, chemical-related diseases, and gene-disease relationships.²⁴ Using default settings, the CTD was used to predict potential targets of asiaticoside. The desired targets were obtained after removing duplicates. The target proteins were then standardized using the Universal Protein Resource (UniProt, <http://www.uniprot.org/>) after being screened from four databases. In parallel, a set of target proteins related to photoaging was established using the GeneCards database, an online resource for exploring gene-disease associations in humans.²⁵

edu.cn/pharmmapper/, is an analytical tool capable of predicting a small molecule's biological targets by comparing it with all the experimentally determined three-dimensional protein structures available on PharmTargetDB.²³ After submitting the 3D structures and using default parameters, PharmMapper predicted the potential targets of asiaticoside. Meanwhile, CTD (<http://ctdbase.org/>) is a freely accessible database that offers curated information on chemical-gene/protein interactions, chemical-related diseases, and gene-disease relationships.²⁴ Using default settings, the CTD was used to predict potential targets of asiaticoside. The desired targets were obtained after removing duplicates. The target proteins were then standardized using the Universal Protein Resource (UniProt, <http://www.uniprot.org/>) after being screened from four databases. In parallel, a set of target proteins related to photoaging was established using the GeneCards database, an online resource for exploring gene-disease associations in humans.²⁵

Target intersection between drugs and diseases

An intersection of Venn diagrams was used to identify the overlapping drug-disease targets by comparing the targets of asiaticoside and those related to photoaging. These targets are considered core targets for the action of asiaticoside in treating photoaging.

Constructing a network of protein-protein interactions (PPIs)

To construct the PPI network, the authors selected the core targets shared by both asiaticoside and photoaging. The STRING database (<https://string-db.org/cgi/input.pl>) is an online resource that provides a comprehensive collection of PPI information from various publicly available sources. In addition to integrating experimental data, the database also incorporates computational predictions to enhance the coverage and accuracy of the PPI network. By integrating and analyzing this wealth of data, the STRING database can provide insights into the functional relationships between proteins and pathways, and facilitate the discovery of novel therapeutic targets. Subsequently, the authors used the core targets as input for STRING to construct a PPI network consisting of interactions between the physical and functional aspects. The confidence score cut-off was set at 0.9 to ensure a high level of confidence in the interactions. The degree of a node in the network, which represents the number of its connections, was used to identify and evaluate the core targets, as well as, the interaction information between nodes. The PPI network was then processed using R language (version 4.1.0), and the top 30 nodes in the network were identified and presented.

Creating the entire network

The authors selected the intersection of PPI nodes for further analysis. Drug-disease relationships and their potential targets were visualized using Cytoscape (version 3.8.0) based on the aforementioned data.²⁶ The connections between each of the nodes represented a biological interaction between the drug, target, or disease. The size of the node was compared to the connectivity analysed by NetworkAnalyzer of Cytoscape associated with the degrees and weight value.²⁷ A larger value indicates a greater possibility of the component being identified as the crucial target of asiaticoside for photoaging.

Gene Ontology (GO) and Kyoto Encyclopedia of Genes and Genomes (KEGG) pathway enrichment analysis

To gain insight into the potential functions of the intersection PPI nodes, a Gene Ontology (GO) analysis was carried out using the clusterProfiler package in the R environment. The analysis focused on three main categories: biological process (BP), molecular func-

tion (MF), and cellular component (CC). By examining the enriched GO terms associated with the target genes, the analysis can provide a deeper understanding of their potential roles in various biological processes and cellular contexts. Such an approach is commonly used in bioinformatics and functional genomics to annotate and interpret large-scale gene or protein datasets.²⁸ Gene list annotation and analysis can be carried out on Metascape (<https://metascape.org/>). Metascape could provide a robust tool for investigating the functional properties of gene lists by incorporating gene annotation, functional enrichment, membership search, and interactome analysis. By integrating over 40 independent knowledge bases, Metascape allows users to access a wealth of information on gene function and regulation, as well as, gain insight into the biological processes and pathways that are associated with their gene lists. Such a platform is widely used in the field of bioinformatics and systems biology to analyze and interpret large-scale genomic and proteomic data.²⁹ Moreover, Metascape can group similar terms and eliminate redundancy, therefore, it was used to carry out the KEGG analysis. To determine the statistical significance of the enrichment analysis, both the *p*-value and adjusted *p*-value were set to a threshold of <0.05. The top 10 enriched GO terms were visualized as a scatter plot and a chord plot was generated to display the 8 most enriched KEGG pathways.

Materials and cell culture

Asiaticoside (Sigma Aldrich, St. Louis, MO, USA, purity >98%) was solubilized beforehand in dimethylsulfoxide. Next, different concentrations of asiaticoside (0, 12.5, 25, 50, 100 and 200 µg/mL) were configured for cell experiments. The final dimethylsulfoxide concentration was controlled to under 0.1%. The authors obtained HDFs with informed written consent from male donors who underwent a routine circumcision process.³⁰ The experiments were carried out using HDFs at passages 3–4 only. This study was approved by the ethics committee of Fudan University School of Medicine (Ethical approval document No: 2022-778).

UVA irradiation

HDFs were cultured in different formats, including 96-well plates (2,000 cells/well for cell proliferation assays) and 10-cm culture dishes (1×10^6 cells for other experiments), in Dulbecco's modified eagle's medium (DMEM, Hyclone, Logan City, UT) supplemented with 10% fetal bovine serum (FBS, Gibco, New Zealand) and 1% antibiotic-antimycotic (Gibco, Grand Island, NY), with or without asiaticoside and Vitamin C (VC; Sigma Aldrich).

After 48 hours of cultivation, the culture medium was replaced with phosphate-buffered saline (PBS) without drugs, and HDFs were exposed to a UVA tube (TL 20W/12, Philips) at various doses (12.5, 25, 50, 100, and 200 mJ/cm²) to determine the appropriate irradiation intensity. Radiation doses were calculated using an ultraviolet intensity meter (Topcon Technohouse Corporation, Tokyo, Japan). After removing the PBS, HDFs were cultured for 48 hours, with or without drugs, in a culture medium. VC of 50 µg/mL served as a positive control.

Cell proliferation assay

To assess cell proliferation, a Cell Counting Kit 8 (CCK-8) assay was performed. HDFs were exposed to varying doses of asiaticoside and subcultured for 48 hours to evaluate the proliferation of cells. Additionally, cell proliferation was measured at 48 hours after exposure to different UVA doses or drug treatments under 100 mJ/cm² UVA irradiation. The results were expressed as the percentage of cell proliferation relative to untreated control HDFs.

RNA extraction and real-time quantitative polymerase chain reaction

RNA was isolated from HDFs 48 hours after irradiation using the EZ-press RNA Purification Kit (EZBioscience, USA). Reverse transcription was performed using a 4×Reverse Transcription Master Mix (EZBioscience) at 42°C for 15 minutes, followed by a 3-minute incubation at 95°C. Next, qPCR was carried out using the 2×SYBR Green qPCR Master Mix (EZBioscience) with an initial denaturation step at 95°C for 5 minutes. Then 40 amplification cycles were performed using a Strata Gene Mx3000p (Applied Biosystems) (10 seconds at 95°C for denaturation and 30 seconds at 60°C for annealing and extension). The primer sequences used for each gene of interest are listed in Table 1. Each gene of interest was normalized to GAPDH, and the fold change was calculated relative to the control. The qPCR assay was performed in triplicate and, as such, repeated three times.

Western blot (WB) assay

Essential proteins selected based on the network pharmacology analysis and *in vitro* experiments were subject to WB assay for further validation. A 4–20% SDS-PAGE gel from Bio-Rad (Hercules, CA) was loaded with 20 µg of protein lysate. The protein fractions were transferred to a nitrocellulose membrane (Bio-Rad) and then the membrane was blocked with 5% bovine serum albumin for one hour. Primary antibodies were added and the membrane was incubated overnight at 4°C. After bathing with a washing buffer, secondary antibodies were added and the membrane was incubated for one hour at room temperature. Protein bands were visualized using an enhanced chemiluminescence detection kit (Thermo Scientific, 32106). To serve as a control, anti-GAPDH was used. Details about all the antibodies used can be found in Table 2.

Asiaticoside-target molecular docking

Following network pharmacology analysis and *in vitro* experiments, molecular docking analysis was used to validate nine core-selected proteins. The three-dimensional structures of the nine targets were obtained from the PDB database (<https://www.rcsb.org/>), while asiaticoside was used as the ligand and the nine targets were used as receptors. The molecular docking analysis was carried out using AutoDock (version 1.5.6). Prior to the docking process, AutoDock was used to prepare the protein targets by removing water molecules, adding nonpolar hydrogen, and isolating the proteins. Gasteiger charges were also calculated to facilitate the docking process. Local Search Parameters were used in AutoDock to perform molecular docking. A conformation with the best affinity was selected, and PyMol (version 2.3) was used to visualize the results.

Statistical analysis

SPSS was used to analyze the experimental data using one-way ANOVA with Tukey's post-hoc test. Differences were considered significant at $p < 0.05$.

Results

Screening of potential drug-disease targets

A total of 246 photoaging-associated targets (Table 3) and 17,292 potential targets for asiaticoside action were acquired (Table S1). After matching the asiaticoside targets with photoaging-related targets, a total of 202 potential asiaticoside targets for treating photoaging were obtained (Fig. 1a and Table 4).

Table 1. Primers used in qPCR analysis

Gene	Primer Sequence (5'-3')	Annealing Temperature (°C)	Product Size (bp)
TGF-β1	Sense: AAGGACCTCGGCTGGAAGTG	58	136
	Antisense: CCGGGTTATGCTGGTTGTA		
TGF-β3	Sense: GGTTTTCCGCTTCAATGTGT	58	119
	Antisense: GCTCGATCCTCTGCTCATT		
TIMP1	Sense: TGACATCCGGTTCTGCTACA	58	102
	Antisense: TGCAGTTTTCCAGCAATGAG		
SMAD4	Sense: CTCATGTGATCTATGCCCGTC	58	146
	Antisense: AGGTGATACAACCTCGTTCGTAGT		
SMAD7	Sense: TCCTCCGCTGAAACAGGG	58	116
	Antisense: CCTCCCAGTATGCCACCAC		
TNF-α	Sense: CTCGAACCCCGAGTGACAAG	58	159
	Antisense: TGAGGTACAGGCCCTCTGAT		
IL-6	Sense: CCTGACCCAACCACAAATGC	58	157
	Antisense: ATCTGAGGTGCCCATGCTAC		
PTEN	Sense: AGGGACGAACTGGTGAATGA	58	100
	Antisense: CTGGTCCTTACTCCCCATAGAA		
PPARγ	Sense: ACCAAAGTGCAATCAAAGTGGGA	58	100
	Antisense: ATGAGGGAGTTGGAAGGCTCT		
PIK3R1	Sense: TGGACGGCGAAGTAAAGCATT	58	154
	Antisense: AGTGTGACATTGAGGGAGTCG		
BCL2L1	Sense: GAGCTGGTGGTTGACTTTCTC	58	119
	Antisense: TCCATCTCCGATTCAGTCCCT		
BAX	Sense: CCCGAGAGGTCTTTTCCGAG	58	155
	Antisense: CCAGCCCATGATGGTTCTGAT		
P53	Sense: GAGTTGGCTCTGACTGTACC	58	133
	Antisense: TCCGTCCCAGTAGATTACCAC		
GAPDH	Sense: ACAACTTTGGTATCGTGAAGG	58	101
	Antisense: GCCATCACGCCACAGTTTC		

BAX, BCL-2-associated X protein; BCL2L1, BCL2 like 1 (human); GAPDH, glyceraldehyde 3-phosphate dehydrogenase; IL-6, interleukin 6; P53, tumor protein p53; PIK3R1, phosphoinositide-3-kinase regulatory subunit 1; PPARγ, peroxisome proliferator-activated receptor gamma; PTEN, phosphatase and tensin homolog; SMAD, suppressor of mothers against decapentaplegic; TGFβ, transforming growth factor-beta; TNF-α, tumour necrosis factor-α.

PPI network of the common targets

To gain insight into asiaticoside's method of action in the treatment of photoaging, it is important to investigate the interactions between the common targets. The authors utilized STRING to construct an interlaced network of the 202 common targets. Next, a network of 171 targets was obtained after removing disconnected nodes as depicted in [Figure 1b](#), and the top 30 targets sorted by R based on degree value was shown in [Figure 1c](#). The researchers postulated that asiaticoside exerts its medicinal effects and treats photoaging by modulating such co-targets.

The construction of the disease-target-drug network

To understand the relationship between the co-targets and drug/disease more intuitively, the “disease-target-drug” network diagram was mapped out using Cytoscape. By intersecting the drug-

disease common targets with the PPI targets, the authors generated a condensed network consisting of 173 nodes including asiaticoside, photoaging, and 171 targets ([Fig. 2a](#)). Next, the authors used the MCC algorithm to evaluate the importance of each node and rank them according to scores ([Fig. 2a](#) and [Table 5](#)).

GO enrichment analyses

As shown in [Figure 2b](#), the 10 top terms about BP, CC and MF were displayed. The color gradient from red to purple represented the trend of increasing p-values and decreasing significance for each term. The BP terms comprised responses, to radiation, light stimulus, UV, oxygen levels, as well as, cellular response to oxidative stress, and response to oxygen levels, among others ([Fig. 2b](#), $p < 0.05$). CC terms included collagen-containing extracellular matrix, RNA polymerase II transcription regula-

Table 2. Antibodies used in western blotting

Targets	Source	Dilution ratio
BAX	Abcam, ab182733	1:2,000
IκB-α	Abcam, ab32518	1:5,000
P-IκBα	Abcam, ab133462	1:10,000
P65	Abcam, ab32536	1:5,000
P-P65	Abcam, ab86299	1:5,000
P53	Abcam, ab26	1:1,000
P-53	Abcam, ab33889	1:2,000
PTEN	Abcam, ab170941	1:5,000
PPARγ	Abcam, ab178860	1:1,000
AKT	Abcam, ab8805	1:500
P-AKT	Abcam, ab8933	1:500
GAPDH	Abcam, ab8245	1:2,000

AKT, protein kinase B; BAX, BCL-2-associated X protein; BCL-2, b-cell lymphoma 2; GAPDH, glyceraldehyde 3-phosphate dehydrogenase; IκBα, nuclear factor of kappa light polypeptide gene enhancer in B-cells inhibitor, alpha; PPARγ, peroxisome proliferator-activated receptor gamma; PTEN, phosphatase and tensin homolog.

tor complex, cornified envelope, and melanosome, and so on (Fig. 2b, $p < 0.05$). Simultaneously, MF terms mainly contained DNA-binding transcription factor binding, collagen binding, nuclear receptor activity, protease binding, as well as, phosphatase binding, and others (Fig. 2b, $p < 0.05$). These GO enrichment results strongly implicated the therapeutic potential of asiaticoside on photoaging.

KEGG enrichment analyses

To gain a comprehensive understanding of the mechanisms underlying the effects of asiaticoside on photoaging, the authors performed KEGG pathway enrichment analyses using Metascape. The top 20 enrichment pathways were obtained and the genes involved in those pathways were listed in Table S2. Based on the results of the top 20 enriched pathways, 8 pathways most strongly associated with photoaging and genes involved in at least 3 of the 8 pathways were screened out for drawing KEGG chord plots, which included pathways in cancer, PI3K-AKT signalling pathway, longevity regulating pathway, NF-κB signalling pathway, TGF-β signalling pathway, melanogenesis, inflammatory mediator regulation of TRP channels, and PPAR signalling pathway (Fig. 2c, $p < 0.05$).

Selection of optimal drug concentration and exposure dosage

To detect the cytotoxicity of asiaticoside, HDFs treated with asiaticoside (0, 12.5, 25, 50, 100 and 200 μg/mL) for 48 h were detected by CCK-8 assay. As shown in Figure 3a, 12.5 and 25 μg/mL asiaticoside improved HDFs proliferation as opposed to the control group ($p < 0.05$), and asiaticoside of 50 μg/mL appeared to have a similar cell proliferation (%) to the control group ($p > 0.05$). However, asiaticoside of 100 and 200 μg/mL had obvious inhibition on the vitality of HDFs, which contributed to over half of the death compared to the control group (Fig. 3a, $p < 0.05$), indicating high concentrations of asiaticoside had cytotoxic effects. Therefore, asiaticoside of 0, 12.5, 25 and 50 μg/mL were selected for the following experiments.

To choose the most appropriate exposure dose of UVA, HDFs

were irradiated by UVA at 0, 12.5, 25, 50, 100 and 200 mJ/cm² respectively, and detected by CCK-8 assay at 48 h post-irradiation. As shown, UVA irradiation significantly inhibited HDFs proliferation at the doses of 25, 50, 100, and 200 mJ/cm² in a dose-dependent manner (Fig. 3b, $p < 0.05$). Among such samples, nearly 50% of HDFs died after being irradiated by UVA of 100 mJ/cm² (Fig. 3b, $p < 0.05$). Hence, UVA of 100 mJ/cm² was selected for the following experiments.

Next, HDFs were segregated into six groups: (1) control group (HDFs untreated by UVA and drugs); (2) UVA group (HDFs exposed to UVA irradiation only); (3) VC group (HDFs exposed to UVA irradiation with VC treatment, serve as a positive control); (4–6) 12.5/25/50 μg/mL asiaticoside group (HDFs exposed to UVA irradiation with 12.5/25/50 μg/mL asiaticoside treatment, respectively).

Asiaticoside rescued UVA-treated HDFs from proliferation inhibition

After pre-treatment with or without VC/asiaticoside for 48 h, HDFs were irradiated by 100 mJ/cm² UVA and then subcultured with VC/asiaticoside for another 48 h. Cell density and proliferation ratio in VC and 25 μg/mL asiaticoside groups could reach a similar level to those of the control group by CCK-8 assay and manual cell counting (Fig. 3c–d, $p < 0.05$).

The experimental results indicated that asiaticoside of 25 μg/mL may have a better effect on preventing adverse cellular response caused by UVA irradiation. Thus, asiaticoside of 25 μg/mL and VC were chosen for subsequent qPCR and WB assay.

Asiaticoside reversed UVA-induced expression of genes and proteins related to photoaging mined by network pharmacology

The researchers chose 13 important core genes sorted by MCC and KEGG pathway enrichment to perform the qPCR assay. TGF-β1 could enhance collagen production and inhibit collagen degradation while TGF-β3 exerts an opposite effect, with each of them playing a crucial role in cellular senescence and aging-related pathology.³¹ As shown in Figure 4, UVA exposure resulted

Table 3. Identification of potential targets for photoaging by GeneCards

MMP1	ELANE	MMP7	CEMIP	DNMT1	ABCC9
ELN	MRC2	RARS1	AKT1	PIK3R1	HRH1
FBN1	FLG	ESR1	CASP3	MMP14	CTSL
JUN	MAPK14	NFKB1	RARB	FN1	KRT19
MC1R	ACACA	MAPK8	ALOX5	HDAC3	TP53BP1
PTGS2	FASN	ESR2	CREB1	NOS2	PRF1
OPN1SW	GLB1	MIF	CDKN1A	NFKBIA	TYRP1
OPN3	SCD	CYP1B1	PIK3CG	SPARC	AGER
FOS	TGM1	HSD17B4	DDB2	TLR4	CLOCK
BMP6	FBLN2	HSD17B2	KRT14	PRKAA2	CCNA2
RARA	LORICRIN	SULT1E1	PPARD	IRAK1	GAL
IVL	CLU	SULT1A1	HYAL1	GNAQ	RPS3
CCN1	HSD11B1	HSD17B8	ANGPT1	STK11	CALCA
MMP3	EGF	GPB1	SHC1	RPS6KB1	DCT
VCAN	POLQ	GREB1	SERPINH1	CASP9	ACP1
MMP9	SPRR1B	TNF	ECM1	ANXA1	ARNTL
MMP2	FBXO40	SOD2	HSF1	CP	POSTN
TRPV1	STXB5L	MYD88	HSPA1A	BAX	TAGLN
KRT16	F2RL1	NR1H2	PTPRK	CYCS	PEX7
CTSD	PDYN	SIRT1	ORAI1	MITF	RPS27A
TIMP1	PLA2G4A	NR1H3	CRABP2	ODC1	TIMP2
TGFBR2	XPA	MMP10	HYAL2	LMNA	IL18R1
IL1R1	MSRA	PPARA	HBEGF	MAPK3	HMMR
TP53	MIR155	GZMB	GDA	NFE2L2	NOX4
MAPK10	LMNB1	KRT17	KRT10	VEGFA	PTPRU
COL1A1	GLO1	SFN	AREG	BCL2L1	FOSB
MYC	HAGH	S100A8	HSPA4	GPX4	GDF15
ITGB1	MSRB1	SIRT4	DUSP16	CYP27B1	MIP
SMAD4	CAT	HYAL3	MFAP2	CYBB	PSMC4
XDH	SOD1	MIR15B	SAA1	HIF1A	TEP1
MIR146A	MMP12	VDR	IL11	KCNJ5	RNASE1
PPARG	SMAD2	RXRA	CSN1S1	LYZ	RBP1
RHO	SMAD7	MMP8	EZH2	RXRB	XAB2
FBN2	CD36	IL1B	MTOR	PTK2	SSBP3
OPN4	IL6	RARG	PRKCD	ATF2	WARS1
OPN5	AQP3	TYR	CTNNA1	COL3A1	DEFB4A
CTSB	IL1A	LOX	CHUK	DHCR7	MIR23A
FAS	EGFR	HAS2	CASP8	TCF7L2	MIR101-1
MMP13	PTEN	MFAP4	MDM2	TGFB3	MIR377

(continued)

Table 3. (continued)

GSR	MAPK1	DSPP	RPS6KA3	ANG	MIR101-2
DCN	TGFB1	IL1RAPL2	CDKN2A	BAD	VTRNA2-1

ABCC9, ATP Binding Cassette Subfamily C Member 9; ACACA, Acetyl-CoA Carboxylase Alpha; ACP1, Acid Phosphatase 1, Soluble; AGER, Advanced Glycosylation End-Product Specific Receptor; AKT1, AKT Serine/Threonine Kinase 1; ALOX5, Arachidonate 5-Lipoxygenase; ANG, Angiogenin; ANGPT1, Angiopoietin 1; ANXA1, Annexin A1; AQP3, Aquaporin 3 (Gill Blood Group); AREG, Amphiregulin; ARNTL, Aryl hydrocarbon receptor nuclear translocator-like protein 1; ATF2, Activating Transcription Factor 2; BAD, BCL2 Associated Agonist Of Cell Death; BAX, BCL2 Associated X, Apoptosis Regulator; BCL2L1, BCL2 Like 1; BMP6, Bone Morphogenetic Protein 6; CALCA, Calcitonin Related Polypeptide Alpha; CASP3, Caspase 3; CASP8, Caspase 8; CASP9, Caspase 9; CAT, Catalase; CCN1, Cellular Communication Network Factor 1; CCNA2, Cyclin A2; CD36, CD36 Molecule; CDKN1A, Cyclin Dependent Kinase Inhibitor 1A; CDKN2A, Cyclin Dependent Kinase Inhibitor 2A; CEMIP, Cell Migration Inducing Hyaluronidase 1; CHUK, Component Of Inhibitor Of Nuclear Factor Kappa B Kinase Complex; CLOCK, Clock Circadian Regulator; CLU, Clusterin, COL1A1, Collagen Type I Alpha 1 Chain; COL3A1, Collagen Type 3 Alpha 1 Chain; CP, Ceruloplasmin; CRABP2, Cellular Retinoic Acid Binding Protein 2; CREB1, CAMP Responsive Element Binding Protein 1; CSN1S1, Casein Alpha S1; CTNNA1, Catenin Beta 1; CTSB, Cathepsin B; CTSD, Cathepsin D; CTSL, Cathepsin L; CYBB, Cytochrome B-245 Beta Chain; CYCS, Cytochrome C, Somatic; CYP11B1, Cytochrome P450 Family 1 Subfamily B Member 1; CYP27B1, Cytochrome P450 Family 27 Subfamily B Member 1; DCN, Decorin; DCT, Dopachrome Tautomerase; DDB2, Damage Specific DNA Binding Protein 2; DEFBA4, Defensin Beta 4A; DHC17, 7-Dehydrocholesterol Reductase; DNMT1, DNA Methyltransferase 1; DSPP, Dentin Sialophosphoprotein; DUSP16, Dual Specificity Phosphatase 16; ECM1, Extracellular Matrix Protein 1; EGF, Epidermal Growth Factor; EGFR, Epidermal Growth Factor Receptor; ELANE, Elastase, Neutrophil Expressed; ELN, Elastin; ESR1, Estrogen Receptor 1; ESR2, Estrogen Receptor 2; EZH2, Enhancer Of Zeste 2 Polycomb Repressive Complex 2 Subunit; F2RL1, F2R Like Trypsin Receptor 1; FAS, Fas Cell Surface Death Receptor; FASN, Fatty Acid Synthase; FBLN2, Fibulin 2; FBN1, Fibrillin 1; FBN2, Fibrillin 2; FBXO40, F-Box Protein 40; FLG, Filaggrin, FN1, Fibronectin 1; FOS, Fos Proto-Oncogene, AP-1 Transcription Factor Subunit; FOSB, FosB Proto-Oncogene, AP-1 Transcription Factor Subunit; GAL, Galanin And GMAP Prepropeptide; GDA, Guanine Deaminase; GDF15, Growth Differentiation Factor 15; GLB1, Galactosidase Beta 1; GLO1, Glyoxalase 1; GNAQ, G Protein Subunit Alpha Q; GPER1, G Protein-Coupled Estrogen Receptor 1; GPX4, Glutathione Peroxidase 4; GREB1, Growth Regulating Estrogen Receptor Binding 1; GSR, Glutathione-Disulfide Reductase; GZMB, Granzyme B; HAGH, Hydroxyacylglutathione Hydrolase; HAS2, Hyaluronan Synthase 2; HBEGF, Heparin Binding EGF Like Growth Factor; HDAC3, Histone Deacetylase 3; HIF1A, Hypoxia Inducible Factor 1 Subunit Alpha; HMMR, Hyaluronan Mediated Motility Receptor; HRH1, Histamine Receptor H1; HSD11B1, Hydroxysteroid 11-Beta Dehydrogenase 1; HSD17B2, Hydroxysteroid 11-Beta Dehydrogenase 2; SD17B4, Hydroxysteroid 11-Beta Dehydrogenase 4; HSD17B8, Hydroxysteroid 11-Beta Dehydrogenase 8; HSF1, Heat Shock Transcription Factor 1; HSPA1A, Heat Shock Protein Family A (Hsp70) Member 1A; HSPA4, Heat Shock Protein Family A (Hsp70) Member 4; HYAL1, Hyaluronidase 1; HYAL2, Hyaluronidase 2; HYAL3, Hyaluronidase 3; IL11, Interleukin 11; IL18R1, Interleukin 18 Receptor 1; IL1A, Interleukin 1 Alpha; IL1B, Interleukin 1 Beta; IL1R1, Interleukin 1 Receptor Type 1; IL1RAPL2, Interleukin 1 Receptor Accessory Protein Like 2; IL6, Interleukin 6; IRAK1, Interleukin 1 Receptor Associated Kinase 1; ITGB1, Integrin Subunit Beta 1; IVL, Involucrin; JUN, Jun proto-oncogene, AP-1 Transcription Factor Subunit; KCNJ5, Potassium Inwardly Rectifying Channel Subfamily J Member 5; KRT10, Keratin 10; KRT14, Keratin 14; KRT16, Keratin 16; KRT17, Keratin 17; KRT19, Keratin 19; LMNA, Lamin A/C; LMNB1, Lamin B1; LORICRIN, Loricrin Cornified Envelope Precursor Protein; LOX, Lysyl Oxidase, LYZ, Lysozyme; MAPK1, Mitogen-Activated Protein Kinase 1; MAPK3, Mitogen-Activated Protein Kinase 3; MAPK8, Mitogen-Activated Protein Kinase 8; MAPK10, Mitogen-Activated Protein Kinase 10; MAPK14, Mitogen-Activated Protein Kinase 14; MC1R, Melanocortin 1 receptor; MDM2, MDM2 Proto-Oncogene; MFAP2, Microfibril Associated Protein 2; MFAP4, Microfibril Associated Protein 4; MIF, Macrophage Migration Inhibitory Factor; MIP, Major Intrinsic Protein Of Lens Fiber; MIR101-1, MicroRNA 101-1; MIR101-2, MicroRNA 101-2; MIR146A, MicroRNA 146a; MIR155, MicroRNA 155; MIR15B, MicroRNA 15B; MIR23A, MicroRNA 23A; MIR377, MicroRNA 377; MITF, Melanocyte Inducing Transcription Factor; MMP1, Matrix Metalloproteinase 1; MMP2, Matrix Metalloproteinase 2; MMP3, Matrix Metalloproteinase 3; MMP7, Matrix Metalloproteinase 7; MMP8, Matrix Metalloproteinase 8; MMP9, Matrix Metalloproteinase 9; MMP10, Matrix Metalloproteinase 10; MMP12, Matrix Metalloproteinase 12; MMP13, Matrix Metalloproteinase 13; MMP14, Matrix Metalloproteinase 14; MRC2, Mannose Receptor C Type 2; MSRA, Methionine Sulfoxide Reductase A; MSRB1, Methionine Sulfoxide Reductase B1; MTOR, Mechanistic Target Of Rapamycin Kinase; MYC, MYC Proto-Oncogene, BHLH Transcription Factor; MYD88, MYD88 Innate Immune Signal Transduction Adaptor; NFE2L2, NFE2 Like BZIP Transcription Factor 2; NFKB1, Nuclear Factor Kappa B Subunit 1; NFKBIA, NFKB Inhibitor Alpha; NOS2, Nitric Oxide Synthase 2; NOX4, NADPH Oxidase 4; NR1H2, Nuclear Receptor Subfamily 1 Group H Member 2; NR1H3, Nuclear Receptor Subfamily 1 Group H Member 3; ODC1, Ornithine Decarboxylase 1; OPN1SW, Opsin 1, Short Wave Sensitive; OPN3, Opsin 3; OPN4, Opsin 4; OPN5, Opsin 5; ORAI1, ORAI Calcium Release-Activated Calcium Modulator 1; PDYN, Prodynorphin; PEX7, Peroxisomal Biogenesis Factor 7; PIK3CG, Phosphatidylinositol-4,5-Bisphosphate 3-Kinase Catalytic Subunit Gamma; PIK3R1, Phosphoinositide-3-Kinase Regulatory Subunit 1; PLA2G4A, Phospholipase A2 Group IVA; POLQ DNA Polymerase Theta; POSTN, Periostin; PPARA, Peroxisome Proliferator Activated Receptor alpha; PPAR, Peroxisome Proliferator Activated Receptor delta; PPARG, Peroxisome Proliferator Activated Receptor Gamma; PRF1, Perforin 1; PRKAA2, Protein Kinase AMP-Activated Catalytic Subunit Alpha 2; PRKCD, Protein Kinase C Delta; PSMC4, Proteasome 26S Subunit, ATPase 4; PTEN, Phosphatase And Tensin Homolog; PTGS2, prostaglandin-endoperoxide synthase 2; PTK2, Protein Tyrosine Kinase 2, PTPRK, Protein Tyrosine Phosphatase Receptor Type K; PTPRU, Protein Tyrosine Phosphatase Receptor Type U; RARA, Retinoic Acid Receptor Alpha; RARB, Retinoic Acid Receptor Beta; RARG, Retinoic Acid Receptor Gamma; RARS1, Arginyl-TRNA Synthetase 1; RBP1, Retinol Binding Protein 1; RHO, Rhodopsin; RNASE1, Ribonuclease A Family Member 1, Pancreatic; RPS27A, Ribosomal Protein S27a; RPS3, Ribosomal Protein S3; RPS6KA3, Ribosomal Protein S6 Kinase A3; RPS6KB1, Ribosomal Protein S6 Kinase B1; RXRA, Retinoid X Receptor Alpha; RXRB, Retinoid X Receptor Beta; S100A8, S100 Calcium Binding Protein A8; SAA1, Serum Amyloid A1; SCD, Stearoyl-CoA Desaturase; SERPINH1, Serpin Family H Member 1; SFN, Stratifin; SHC1, SHC Adaptor Protein 1; SIRT1, Sirtuin 1; SIRT4, Sirtuin 4; SMAD2, SMAD Family Member 2; SMAD4, SMAD Family Member 4; SMAD7, SMAD Family Member 7; SOD1, Superoxide Dismutase 1; SOD2, Superoxide Dismutase 2; SPARC, Secreted Protein Acidic And Cysteine Rich; SPRR1B, Small Proline Rich Protein 1B; SSBP3, Single Stranded DNA Binding Protein 3; STK11, Serine/Threonine Kinase 11; STXBPSL, Syntaxin Binding Protein 5L; SULT1A1, Sulfotransferase Family 1A Member 1; SULT1E1, Sulfotransferase Family 1E Member 1; TAGLN, Transglin, TCF7L2, Transcription Factor 7 Like 2; TEP1, Telomerase Associated Protein 1; TGFB1, Transforming Growth Factor Beta 1; TGFB3, Transforming Growth Factor Beta 3; TGFB2, Transforming Growth Factor Beta Receptor 2; TGM1, Transglutaminase 1; TIMP1, Tissue Inhibitor of the Metalloproteinases 1; TIMP2, Tissue Inhibitor of the Metalloproteinases 2; TLR4, Toll Like Receptor 4; TNF, Tumor Necrosis Factor; TP53, Tumor Protein P53; TP53BP1, Tumor Protein P53 Binding Protein 1; TRPV1, Transient Receptor Potential Cation Channel Subfamily V Member 1; TYR, Tyrosinase; TYRP1, Tyrosinase Related Protein 1; VCAN, Versican; VDR, Vitamin D Receptor; VEGFA, Vascular Endothelial Growth Factor A; VTRNA2-1, Vault RNA 2-1; WARS1, Tryptophanyl-TRNA Synthetase 1; XAB2, XPA Binding Protein 2; XDH, Xanthine Dehydrogenase; XPA, DNA Damage Recognition And Repair Factor.

in a significantly reduced TGF- β 1 and increased TGF- β 3 expression than the control group ($p < 0.05$), but a rescuing effect was found in VC and 25 μ g/mL asiaticoside treatment groups. TIMP1 is a natural inhibitor of MMPs stimulating fibroblast proliferation, collagen, and ECM production.³² Activation of SMAD4 and inhibition of SMAD7 could promote TGF- β /Smad signalling pathway which prevents the cells from photoaging and promotes photoaging skin cell repair.³³ Apparent decline in TIMP1 and SMAD4 gene expressions and increased gene expression of SMAD7 were displayed after UVA irradiation compared to the control group (Fig. 4a, $p < 0.05$). However, both VC and 25 μ g/mL asiaticoside retracted the abnormal expression of TIMP1, SMAD4, and SMAD7 to a similar level compared to the control group (Fig.

4a, $p > 0.05$).

Activated NF- κ B signalling pathway in the photoaging process results in a significant inflammatory response accelerating skin photoaging by secretion of multiple pro-inflammatory cytokines.³ IL-6 and TNF- α are the downstream signalling factors and essential activators of the NF- κ B pathway.³⁴ A qPCR analysis revealed remarkably upregulated gene expressions of IL-6 and TNF- α in HDFs exposed to UVA as opposed to the control group (Fig. 4a, $p < 0.05$). However, treatment of VC and asiaticoside abolished IL-6 and TNF- α expression at different levels than the UVA group (Fig. 4a, $p < 0.05$), and rescued the expression levels similar to the control group (Fig. 4a, $p > 0.05$).

PTEN and PPAR γ are known significant negative regulators of

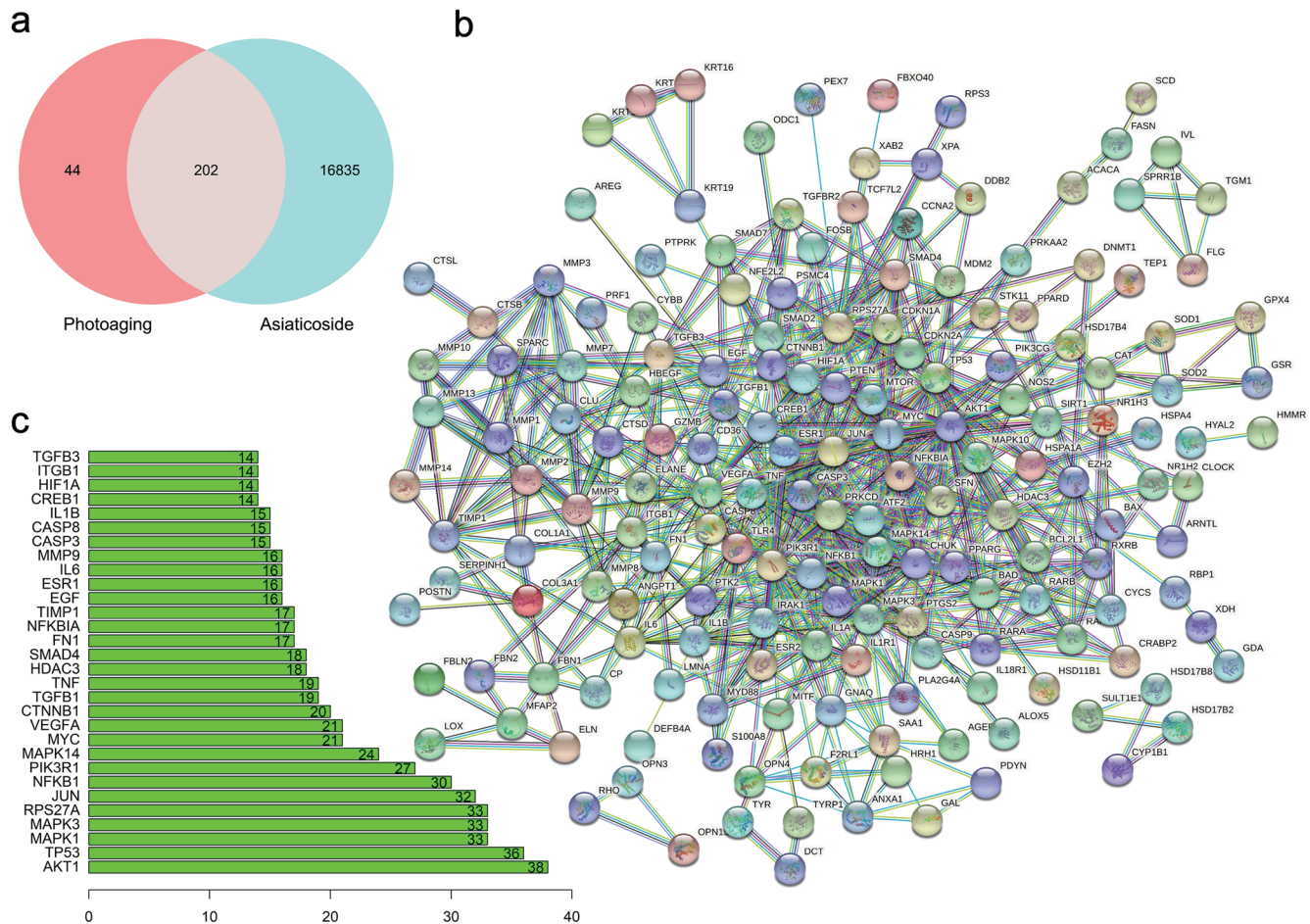


Fig. 1. Examination of shared targets between photoaging and asiaticoside. (a) Venn diagram showing the overlap of targets related to photoaging and asiaticoside. (b) Protein-protein interaction (PPI) network of common targets between photoaging and asiaticoside. (c) Top 30 shared targets ranked by degree values. AKT1, AKT Serine/Threonine Kinase 1; CASP, Caspase; CREB1, CAMP Responsive Element Binding Protein 1; CTNNB1, Catenin Beta 1; EGF, Epidermal Growth Factor; ESR1, Estrogen Receptor 1; FN1, Fibronectin 1; HDAC3, Histone Deacetylase 3; HIF1A, Hypoxia Inducible Factor 1 Subunit Alpha; IL1B, Interleukin 1 Beta; IL6, Interleukin 6; JUN, Jun proto-oncogene, AP-1 Transcription Factor Subunit; MAPK, Mitogen-Activated Protein Kinase; MMP9, Matrix Metalloproteinase 9; NFKB1, Nuclear Factor Kappa B Subunit 1; NFKB1A, NFKB Inhibitor Alpha; PIK3R1, Phosphoinositide-3-Kinase Regulatory Subunit 1; RPS27A, Ribosomal Protein S27a; SMAD4, SMAD Family Member 4; TGB1, Integrin Subunit Beta 1; TGFB1, Transforming Growth Factor Beta 1; TGFB3, Transforming Growth Factor Beta 3; TIMP1, Tissue Inhibitor of the Metalloproteinases 1; TNF, Tumor Necrosis Factor; TP53, Tumor Protein P53; VEGFA, Vascular Endothelial Growth Factor A.

PI3K-AKT signalling, which is suppressed in photoaging and accompanied by a decreased expression of p-AKT that leads to cell apoptosis.⁴ PIK3R1 encodes the regulatory subunit of the PI3K heterodimer which contributes to the PI3K activity.³⁵ Pro-apoptotic BAX, P53 and anti-apoptotic BCL2L1 are strictly related to the PI3K-AKT pathway.^{36,37} As shown in Figure 4, UVA irradiation could markedly upregulate mRNA expression of PTEN, PPAR γ , BAX, and P53 and downregulates PIK3R1 and BCL2L1 expression as opposed to the control group ($p < 0.05$). But the treatment of VC and 25 $\mu\text{g}/\text{mL}$ asiaticoside could rescue UVA-induced gene expressions, especially the asiaticoside group that showed no significant expression difference of PTEN, PPAR γ , BAX, P53, and BCL2L1, including an upregulated expression of PIK3R1 compared to the control group (Fig. 4a, $p < 0.05$).

WB assay was used for further validation. As shown in Figure 4b, an increased ratio of p-P65/P65 and p-I κ B α /I κ B α in HDFs was detected in UVA-irradiated HDFs implicating the activation of the NF- κ B pathway. But such phenomenon can be attenuated

by VC and reversed by 25 $\mu\text{g}/\text{mL}$ asiaticoside treatment (Fig. 4b). Corresponding to the qPCR results, UVA irradiation stimulated the protein expression levels of BAX, PTEN, and PPAR γ compared to the control group (Fig. 4b). However treatment by VC and asiaticoside could counteract the stimulation (Fig. 4b). Similarly, the downregulated ratio of p-AKT/AKT in UVA-irradiated HDFs revealed the suppression of PI3K-AKT pathway (Fig. 4b). However, the suppressed effect was reversed by VC and asiaticoside (Fig. 4b). Although no expressed difference of P53 was observed in the UVA and control groups, p-P53 which is more stable and had an increased activity compared to P53 had a significantly increased expression after UVA irradiation than that of the control group (Fig. 4b). Unexpectedly, drug treatment could rescue the upregulated p-P53 and the effect in asiaticoside group was more pronounced (Fig. 4b).

The results indicated that asiaticoside might rescue UVA-induced photoaging by preventing ECM degradation, repressing inflammatory response, and inhibiting cell apoptosis.

Table 4. Co-targeted genes for photoaging and asiaticoside

BCL2L1	SIRT1	RPS27A	SPRR1B	FBN1
HSD11B1	OPN3	ELANE	PRKAA2	CDKN2A
JUN	GPX4	MYC	HDAC3	CTSL
CAT	NFKB1	MC1R	FN1	MIP
MAPK14	IL1R1	GLO1	ECM1	IL11
MTOR	FBXO40	ARNTL	MFAP2	HSPA4
RARG	SMAD4	ACACA	TAGLN	IL6
HBEGF	MAPK1	PIK3CG	HAS2	RPS3
RARB	ANG	LOX	S100A8	HYAL2
MMP1	TGFB1	IL1B	MAPK10	CTSB
MMP13	CD36	CASP9	SOD1	KRT16
CRABP2	NR1H3	TGFBR2	HYAL3	MRC2
CCNA2	SFN	SULT1A1	SMAD2	ALOX5
PPARG	PTEN	MMP7	MMP10	RNASE1
MMP3	CASP3	GNAQ	BAX	COL1A1
RARA	SAA1	CSN1S1	IL1A	SOD2
PRKCD	MIF	GDF15	TYR	BAD
ESR1	SIRT4	SPARC	F2RL1	KCNJ5
FASN	MMP14	CLU	HSPA1A	RBP1
ANXA1	FOSB	ORAI1	POLQ	PSMC4
DNMT1	CYCS	POSTN	HYAL1	XAB2
ESR2	PRF1	BMP6	NR1H2	MYD88
TRPV1	TEP1	ATF2	HRH1	TGFB3
TNF	NFKBIA	CYBB	CP	RHO
MMP9	SULT1E1	TGM1	CDKN1A	ODC1
NOS2	MMP12	MSRA	SMAD7	SSBP3
PLA2G4A	FBLN2	HSD17B4	HIF1A	SCD
EGF	GZMB	HMMR	IL1RAPL2	CEMIP
PTGS2	MITF	ITGB1	MMP8	LMNA
DCT	KRT10	SERPINH1	CLOCK	CTSD
RXRβ	STXBPSL	NFE2L2	IRAK1	DDB2
AKT1	TP53	MAPK3	TYRP1	CHUK
GSR	HSD17B2	PIK3R1	ABCC9	PTK2
CASP8	STK11	TIMP1	MDM2	HSD17B8
KRT19	KRT14	XPA	PPARD	GAL
CYP1B1	PTPRU	AQP3	AREG	AGER
FLG	TLR4	ELN	CREB1	CTNNB1
PEX7	OPN4	IVL	EZH2	GDA
PTPRK	OPN1SW	MMP2	VEGFA	DEFB4A

(continued)

Table 4. (continued)

PDYN	COL3A1	ANGPT1	TCF7L2	FBN2
XDH	IL18R1			

ABCC9, ATP Binding Cassette Subfamily C Member 9; ACACA, Acetyl-CoA Carboxylase Alpha; AGER, Advanced Glycosylation End-Product Specific Receptor; AKT1, AKT Serine/Threonine Kinase 1; ALOX5, Arachidonate 5-Lipoxygenase; ANG, Angiogenin; ANGPT1, Angiotensinogen 1; ANXA1, Annexin A1; AQP3, Aquaporin 3 (Gill Blood Group); AREG, Amphiregulin; ARNTL, Aryl hydrocarbon receptor nuclear translocator-like protein 1; ATF2, Activating Transcription Factor 2; BAD, BCL2 Associated Agonist Of Cell Death; BAX, BCL2 Associated X, Apoptosis Regulator; BCL2L1, BCL2 Like 1; BMP6, Bone Morphogenetic Protein 6; CASP3, Caspase 3; CASP8, Caspase 8; CASP9, Caspase 9; CAT, Catalase; CCNA2, Cyclin A2; CD36, CD36 Molecule; CDKN1A, Cyclin Dependent Kinase Inhibitor 1A; CDKN2A, Cyclin Dependent Kinase Inhibitor 2A; CEMIP, Cell Migration Inducing Hyaluronidase 1; CHUK, Component Of Inhibitor Of Nuclear Factor Kappa B Kinase Complex; CLOCK, Clock Circadian Regulator; CLU, Clusterin, COL1A1, Collagen Type I Alpha 1 Chain; COL3A1, Collagen Type 3 Alpha 1 Chain; CP, Ceruloplasmin; CRABP2, Cellular Retinoic Acid Binding Protein 2; CREB1, CAMP Responsive Element Binding Protein 1; CSN1S1, Casein Alpha S1; CTNNA1, Catenin Beta 1; CTSB, Cathepsin B; CTSD, Cathepsin D; CTSL, Cathepsin L; CYBB, Cytochrome B-245 Beta Chain; CYCS, Cytochrome C, Somatic; CYP11B1, Cytochrome P450 Family 1 Subfamily B Member 1; DCT, Dopachrome Tautomerase; DDB2, Damage Specific DNA Binding Protein 2; DEFB4A, Defensin Beta 4A; DNMT1, DNA Methyltransferase 1; ECM1, Extracellular Matrix Protein 1; EGF, Epidermal Growth Factor; ELANE, Elastase, Neutrophil Expressed; ELN, Elastin; ESR1, Estrogen Receptor 1; ESR2, Estrogen Receptor 2; EZH2, Enhancer Of Zeste 2 Polycomb Repressive Complex 2 Subunit; F2RL1, F2R Like Trypsin Receptor 1; FASN, Fatty Acid Synthase; FBLN2, Fibulin 2; FBN1, Fibrillin 1; FBN2, Fibrillin 2; FBXO40, F-Box Protein 40; FLG, Filaggrin, FN1, Fibronectin 1; FOSB, FosB Proto-Oncogene, AP-1 Transcription Factor Subunit; GAL, Galanin And GMAP Prepropeptide; GDA, Guanine Deaminase; GDF15, Growth Differentiation Factor 15; GLO1, Glyoxalase 1; GNAQ, G Protein Subunit Alpha Q; GPX4, Glutathione Peroxidase 4; GSR, Glutathione-Disulfide Reductase; GZMB, Granzyme B; HAS2, Hyaluronan Synthase 2; HBEGF, Heparin Binding EGF Like Growth Factor; HDAC3, Histone Deacetylase 3; HIF1A, Hypoxia Inducible Factor 1 Subunit Alpha; HMMR, Hyaluronan Mediated Motility Receptor; HRH1, Histamine Receptor H1; HSD11B1, Hydroxysteroid 11-Beta Dehydrogenase 1; HSD17B2, Hydroxysteroid 11-Beta Dehydrogenase 2; SD17B4, Hydroxysteroid 11-Beta Dehydrogenase 4; HSD17B8, Hydroxysteroid 11-Beta Dehydrogenase 8; HSF1, Heat Shock Transcription Factor 1; HSPA1A, Heat Shock Protein Family A (Hsp70) Member 1A; HSPA4, Heat Shock Protein Family A (Hsp70) Member 4; HYAL1, Hyaluronidase 1; HYAL2, Hyaluronidase 2; HYAL3, Hyaluronidase 3; IL11, Interleukin 11; IL18R1, Interleukin 18 Receptor 1; IL1A, Interleukin 1 Alpha; IL1B, Interleukin 1 Beta; IL1R1, Interleukin 1 Receptor Type 1; IL1RAPL2, Interleukin 1 Receptor Accessory Protein Like 2; IL6, Interleukin 6; IRAK1, Interleukin 1 Receptor Associated Kinase 1; ITGB1, Integrin Subunit Beta 1; IVL, Involucrin; JUN, Jun proto-oncogene, AP-1 Transcription Factor Subunit; KCNJ5, Potassium Inwardly Rectifying Channel Subfamily J Member 5; KRT10, Keratin 10; KRT14, Keratin 14; KRT16, Keratin 16; KRT19, Keratin 19; LMNA, Lamin A/C; LOX, Lysyl Oxidase, LYZ, Lysozyme; MAPK1, Mitogen-Activated Protein Kinase 1; MAPK3, Mitogen-Activated Protein Kinase 3; MAPK10, Mitogen-Activated Protein Kinase 10; MAPK14, Mitogen-Activated Protein Kinase 14; MC1R, Melanocortin 1 receptor; MDM2, MDM2 Proto-Oncogene; MFAP2, Microfibril Associated Protein 2; MIF, Macrophage Migration Inhibitory Factor; MIP, Major Intrinsic Protein Of Lens Fiber; MITF, Melanocyte Inducing Transcription Factor; MMP1, Matrix Metalloproteinase 1; MMP2, Matrix Metalloproteinase 2; MMP3, Matrix Metalloproteinase 3; MMP7, Matrix Metalloproteinase 7; MMP8, Matrix Metalloproteinase 8; MMP9, Matrix Metalloproteinase 9; MMP10, Matrix Metalloproteinase 10; MMP12, Matrix Metalloproteinase 12; MMP13, Matrix Metalloproteinase 13; MMP14, Matrix Metalloproteinase 14; MRC2, Mannose Receptor C Type 2; MSRA, Methionine Sulfoxide Reductase A; MTOR, Mechanistic Target Of Rapamycin Kinase; MYC, MYC Proto-Oncogene, BHLH Transcription Factor; MYD88, MYD88 Innate Immune Signal Transduction Adaptor; NFE2L2, NFE2 Like BZIP Transcription Factor 2; NFKB1, Nuclear Factor Kappa B Subunit 1; NFKBIA, NFKB Inhibitor Alpha; NOS2, Nitric Oxide Synthase 2; NR1H2, Nuclear Receptor Subfamily 1 Group H Member 2; NR1H3, Nuclear Receptor Subfamily 1 Group H Member 3; ODC1, Ornithine Decarboxylase 1; OPN1SW, Opsin 1, Short Wave Sensitive; OPN3, Opsin 3; OPN4, Opsin 4; ORAI1, ORAI Calcium Release-Activated Calcium Modulator 1; PDYN, Prodynorphin; PEX7, Peroxisomal Biogenesis Factor 7; PIK3CG, Phosphatidylinositol-4,5-Bisphosphate 3-Kinase Catalytic Subunit Gamma; PIK3R1, Phosphoinositide-3-Kinase Regulatory Subunit 1; PLA2G4A, Phospholipase A2 Group IVA; POLQ, DNA Polymerase Theta; POSTN, Periostin; PPAR, Peroxisome Proliferator Activated Receptor delta; PPARG, Peroxisome Proliferator Activated Receptor Gamma; PRF1, Perforin 1; PRKAA2, Protein Kinase AMP-Activated Catalytic Subunit Alpha 2; PRKCD, Protein Kinase C Delta; PSMC4, Proteasome 26S Subunit, ATPase 4; PTEN, Phosphatase And Tensin Homolog; PTGS2, prostaglandin-endoperoxide synthase 2; PTK2, Protein Tyrosine Kinase 2, PTPRK, Protein Tyrosine Phosphatase Receptor Type K; PTPRU, Protein Tyrosine Phosphatase Receptor Type U; RARA, Retinoic Acid Receptor Alpha; RARB, Retinoic Acid Receptor Beta; RARG, Retinoic Acid Receptor Gamma; RARS1, Arginyl-tRNA Synthetase 1; RBP1, Retinol Binding Protein 1; RHO, Rhodopsin; RNASE1, Ribonuclease A Family Member 1, Pancreatic; RPS27A, Ribosomal Protein S27a; RPS3, Ribosomal Protein S3; RXRB, Retinoid X Receptor Beta; S100A8, S100 Calcium Binding Protein A8; SAA1, Serum Amyloid A1; SCD, Stearoyl-CoA Desaturase; SERPINH1, Serpin Family H Member 1; SFN, Stratifin; SIRT1, Sirtuin 1; SIRT4, Sirtuin 4; SMAD2, SMAD Family Member 2; SMAD4, SMAD Family Member 4; SOD1, Superoxide Dismutase 1; SOD2, Superoxide Dismutase 2; SPARC, Secreted Protein Acidic And Cysteine Rich; SPRR1B, Small Proline Rich Protein 1B; SSBP3, Single Stranded DNA Binding Protein 3; STK11, Serine/Threonine Kinase 11; STXBPSL, Syntaxin Binding Protein 5L; SULT1A1, Sulfotransferase Family 1A Member 1; SULT1E1, Sulfotransferase Family 1E Member 1; TAGLN, Transgelin, TCF7L2, Transcription Factor 7 Like 2; TEP1, Telomerase Associated Protein 1; TGFB1, Transforming Growth Factor Beta 1; TGFB3, Transforming Growth Factor Beta 3; TGFB2, Transforming Growth Factor Beta Receptor 2; TGM1, Transglutaminase 1; TIMP1, Tissue Inhibitor of the Metalloproteinases 1; TLR4, Toll-Like Receptor 4; TNF, Tumor Necrosis Factor; TP53, Tumor Protein P53; TRPV1, Transient Receptor Potential Cation Channel Subfamily V Member 1; TYR, Tyrosinase; TYRP1, Tyrosinase Related Protein 1; VEGFA, Vascular Endothelial Growth Factor A; XAB2, XPA Binding Protein 2; XDH, Xanthine Dehydrogenase; XPA, DNA Damage Recognition And Repair Factor.

Results of molecular docking

A comprehensive consideration of the core targets sorted by MCC analysis and participation in the core signalling pathways was invalidated by *in vitro* experiments. Molecular docking analysis was conducted on a total of 9 molecules. The results indicated that asiaticoside displayed a high binding affinity with the selected targets BAX, PIK3R1, PTEN, PPAR γ , P53, TNF- α , TGF- β 1, TGF- β 3, and SMAD4. As shown in Figure 5, in the formation of various hydrogen bonds with residues at very close distances, asiaticoside established a stable complex with the selected target proteins.

Discussion

Skin aging could be attributed to chronological aging and UV-induced photoaging. A leading cause of premature photoaging was UV (especially UVA) exposure, appearing as photodamage superimposed on the aging process, characterized by sagging, fragility, dyspigmentation, wrinkles, skin roughness, and decreased skin flexibility.^{1,2}

A study demonstrated that inflammation and apoptosis were the major hallmarks of skin photoaging.³⁸ UVA-induced oxidative stress triggered the overproduction of ROS and caused a variety of damage to fibroblasts including excessive inflammatory response.³⁹ Moreover, UVA promoted photoaging and inflammatory infiltration in the skin and in turn, the inflammatory response accelerated the process of photoaging.⁴⁰ Exposure to UV also led to mass cell apoptosis, both skin barrier and function disruption, as well as, accelerated photoaging.⁴¹

Currently, various strategies have been employed to maintain the structure and function of skin during photoaging, including antioxidant products, stem cell therapies, and intense pulsed light, among others.^{42,43} Plant extracts with proven antioxidant, anti-inflammatory and anti-apoptotic properties have been increasingly explored to prevent or reduce skin damage caused by oxidative stress, such as skin cancer and photoaging.^{44,45} Asiaticoside is a traditional Chinese herbal monomer that has been used for many years to treat various skin diseases like skin ulcer and scleroderma.^{14,15} Asiaticoside possesses diverse pharmacological effects, including antioxidant activity including the ability to scavenge free radicals, as well as, anti-apoptotic, anti-inflammatory, and anti-

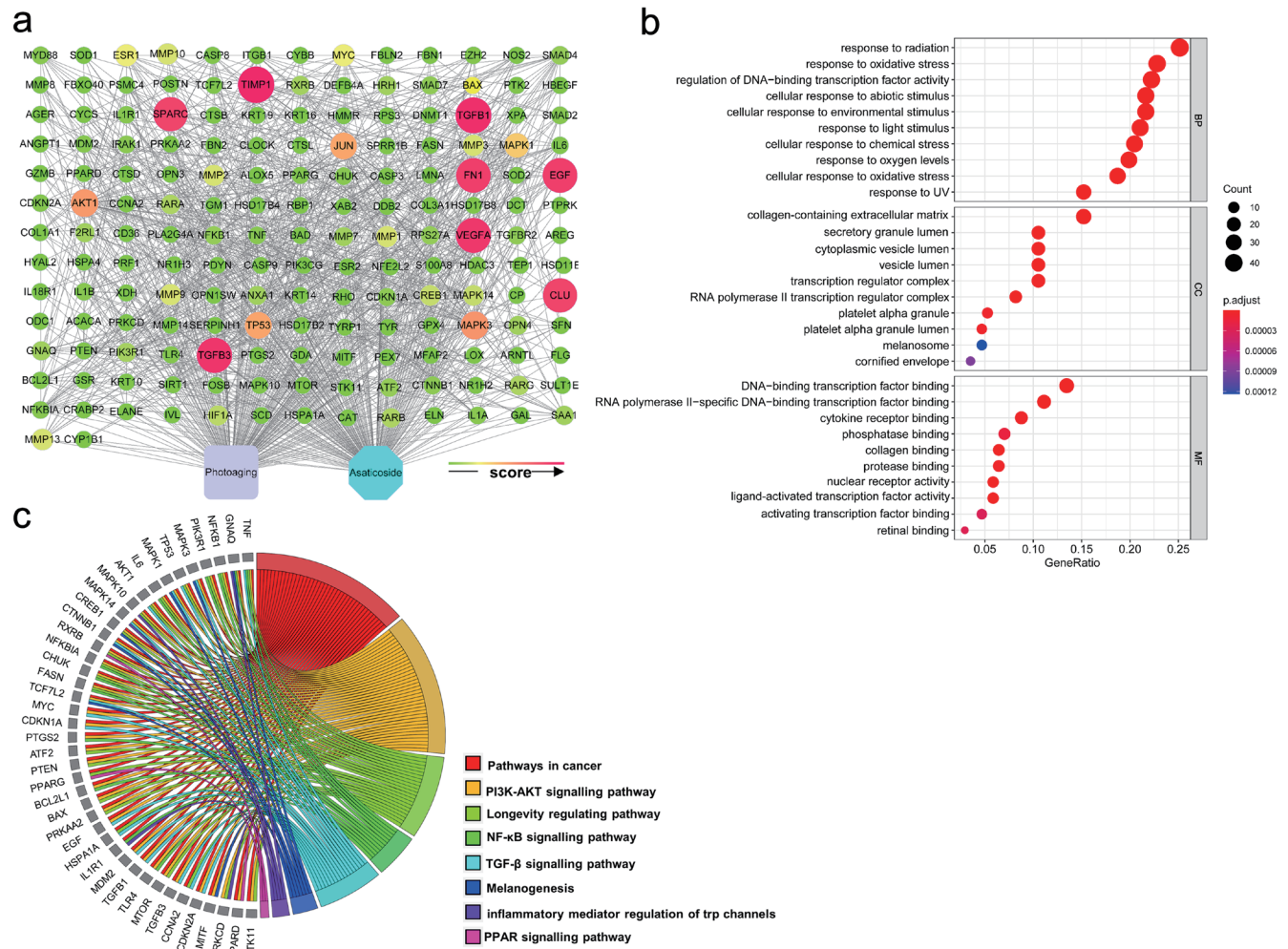


Fig. 2. Enrichment analysis of the core targets. (a) Relationship between photoaging, asiaticoside, and common targets, visualized using Cytoscape. Proteins are ranked by the Matthews correlation coefficient (MCC) score. (b) Gene Ontology (GO) enrichment analysis of core targets, including biological processes (BP), molecular functions (MF), and cellular components (CC). (c) Kyoto Encyclopedia of Genes and Genomes (KEGG) pathway enrichment analysis of core targets. Pathways are on the right side of the chord plot, while genes are on the left side. The corresponding colour of the gene ribbon is consistent with the colour of terms, indicating that this gene is enriched in this term. NF- κ B, nuclear factor kappa-light-chain-enhancer of activated B cells; PI3K-AKT, phosphatidylinositol 3 kinase-protein kinase B; PPAR, peroxisome proliferator-activated receptor; TGF β , transforming growth factor-beta; UV, ultraviolet.

tumor activities.^{16,17} Thus, it was hypothesized that asiaticoside may confer protective effects against photoaging induced by UVA radiation.

In this study, core targets and significantly enriched 8 signalling pathways were identified by network pharmacology analyses which provided a preliminary validation of asiaticoside efficacy on photoaging (Figs. 1–2). Previous studies found that UVA irradiation disrupted cellular fractions by overproduction of ROS, which induced macromolecule damage and accelerated skin aging, as well as, cancer.² ROS accumulation and cell aging could regulate the longevity regulation pathway⁵ and stimulate the TGF- β /Smad pathway.⁶ In addition, ROS could activate NF- κ B signalling pathway and result in severe inflammatory responses of affected skin.³ PI3K-AKT signalling pathway could also be suppressed by ROS, which led to cell apoptosis.⁴ Moreover, enhanced MAPK and PPAR signalling could lead to decreased collagen and TIMP1 production under UVA irradiation^{8,46} and UVA irradiation was revealed to promote the development of both

nonmelanoma skin cancer, as well as, melanoma,⁴⁷ including the activation of TRPV2 by oxidizing.⁴⁸ Such results reported above proved the accuracy of our network pharmacology analysis.

After establishing a successful *in vitro* model, the authors contended that asiaticoside indeed prevented photoaging by reversing UVA-induced HDFs proliferation inhibition (Fig. 3). Moreover, 25 μ g/mL asiaticoside appeared to rank the best photoprotective effect (Fig. 3). Both qPCR and WB were employed to elucidate the mechanisms of asiaticoside on photoaging. As the authors recognize, photoaged skin is marked by increased degradation and turnover of ECM with overexpressed MMPs, and down-expressed TIMP1, which is triggered by the attenuated TGF- β /Smad pathway.⁷ The researchers' network pharmacology analysis revealed TGF- β 1, TGF- β 3, TIMP1, MMP1, MMP2, MMP3, MMP9, MMP13, SMAD4, and SMAD7 are the core targets in the drug-disease-target network and TGF- β signalling pathway was significantly enriched in KEGG pathways (Fig. 1–2, Table 5 and S2). A qPCR indicated that 25 μ g/mL asiaticoside and 50 μ g/mL VC could

Table 5. The information of core targets by MCC analysis

Rank	Name	Score	Rank	Name	Score
1	Photoaging	96,552	88	ELANE	108
1	Asiaticoside	96,552	89	SOD2	96
3	TIMP1	91,248	89	ESR2	96
4	TGFB1	88,812	91	HSPA1A	76
5	TGFB3	85,680	92	HSD17B4	72
6	VEGFA	84,888	92	NR1H3	72
7	EGF	82,732	94	CTSD	68
8	FN1	82,680	95	HBEGF	64
9	SPARC	80,700	96	SOD1	60
10	CLU	80,640	96	MMP8	60
11	MAPK3	52,200	96	STK11	60
12	AKT1	50,576	99	COL3A1	52
13	TP53	46,740	99	KRT19	52
14	JUN	46,192	99	ANGPT1	52
15	MAPK1	36,012	102	SPRR1B	48
16	ESR1	23,608	102	IVL	48
17	MYC	23,448	102	LMNA	48
18	MMP9	20,464	102	NR1H2	48
19	MMP2	20,368	102	S100A8	48
20	MMP3	20,220	102	KRT10	48
21	MMP13	20,208	102	KRT14	48
22	MMP1	20,172	102	KRT16	48
23	MMP10	20,160	102	GAL	48
24	CREB1	17,440	102	PDYN	48
25	MAPK14	17,240	102	FOSB	48
26	HIF1A	15,364	102	BAX	48
27	RARA	12,480	102	MMP14	48
27	RARB	12,480	102	COL1A1	48
27	RARG	12,480	102	FLG	48
30	PIK3R1	11,112	102	TGM1	48
31	RXRβ	10,624	118	PLA2G4A	40
32	SAA1	10,380	118	MFAP2	40
33	GNAQ	10,152	120	GSR	24
34	ANXA1	10,128	120	CD36	24
35	MMP7	10,104	120	GPX4	24
36	F2RL1	10,080	120	DDB2	24
36	OPN4	10,080	120	XPA	24
36	HRH1	10,080	120	DNMT1	24
39	SMAD4	7,572	120	ARNTL	24
40	ATF2	7,488	120	CLOCK	24

(continued)

Table 5. (continued)

Rank	Name	Score	Rank	Name	Score
41	NFKB1	7,180	120	ELN	24
42	RPS27A	7,008	120	FBN2	24
43	SMAD7	5,760	130	PRKAA2	20
43	TGFBR2	5,760	130	GZMB	20
45	CDKN1A	5,136	132	PPARD	16
46	CTNNB1	4,800	133	OPN1SW	12
47	IRAK1	4,128	133	OPN3	12
48	MYD88	3,648	133	RHO	12
49	IL1A	3,408	133	SERPINH1	12
50	TNF	3,276	133	XAB2	12
51	CHUK	3,264	133	NFE2L2	12
52	SMAD2	2,988	133	PIK3CG	12
53	IL1R1	2,928	133	PTPRK	12
54	IL1B	2,884	133	LOX	12
55	NFKBIA	2,748	142	XDH	8
56	MDM2	2,448	142	CYBB	8
56	HDAC3	2,448	142	ACACA	8
58	CDKN2A	2,112	142	FASN	8
59	EZH2	1,980	142	SULT1E1	8
60	TLR4	1,732	142	IL18R1	8
61	ITGB1	1,716	142	RBP1	8
62	PPARG	1,612	142	CTSB	8
63	IL6	1,488	142	CYP1B1	8
64	BCL2L1	1,248	142	HSD17B2	8
65	CASP8	1,080	142	HSD17B8	8
66	CASP3	876	142	DCT	8
67	PSMC4	784	142	TYR	8
68	PTEN	648	142	TYRP1	8
68	BAD	648	156	GDA	4
70	SFN	516	156	PRF1	4
71	CCNA2	480	156	ODC1	4
72	PRKCD	456	156	PEX7	4
73	NOS2	420	156	HMMR	4
74	MTOR	316	156	HYAL2	4
75	CYCS	304	156	HSD11B1	4
76	FBN1	300	156	HSPA4	4
77	CASP9	288	156	POSTN	4
77	PTK2	288	156	TEP1	4
79	MAPK10	264	156	RPS3	4
80	AGER	240	156	CTSL	4

(continued)

Table 5. (continued)

Rank	Name	Score	Rank	Name	Score
80	CP	240	156	ALOX5	4
80	CRABP2	240	156	DEFB4A	4
80	TCF7L2	240	156	AREG	4
84	MITF	152	156	SCD	4
85	SIRT1	144	156	FBLN2	4
86	PTGS2	128	156	FBXO40	4
87	CAT	124			

ACACA, Acetyl-CoA Carboxylase Alpha; AGER, Advanced Glycosylation End-Product Specific Receptor; AKT1, AKT Serine/Threonine Kinase 1; ALOX5, Arachidonate 5-Lipoxygenase; ANGPT1, Angiotensinogen 1; ANXA1, Annexin A1; AREG, Amphiregulin; ARNTL, Aryl hydrocarbon receptor nuclear translocator-like protein 1; ATF2, Activating Transcription Factor 2; BAD, BCL2 Associated Agonist Of Cell Death; BAX, BCL2 Associated X, Apoptosis Regulator; BCL2L1, BCL2 Like 1; CASP3, Caspase 3; CASP8, Caspase 8; CASP9, Caspase 9; CAT, Catalase; CCNA2, Cyclin A2; CD36, CD36 Molecule; CDKN1A, Cyclin Dependent Kinase Inhibitor 1A; CDKN2A, Cyclin Dependent Kinase Inhibitor 2A; CHUK, Component Of Inhibitor Of Nuclear Factor Kappa B Kinase Complex; CLOCK, Clock Circadian Regulator; CLU, Clusterin, COL1A1, Collagen Type I Alpha 1 Chain; COL3A1, Collagen Type 3 Alpha 1 Chain; CP, Ceruloplasmin; CRABP2, Cellular Retinoic Acid Binding Protein 2; CREB1, CAMP Responsive Element Binding Protein 1; CTNNB1, Catenin Beta 1; CTSB, Cathepsin B; CTSN, Cathepsin D; CTSL, Cathepsin L; CYBB, Cytochrome B-245 Beta Chain; CYCS, Cytochrome C, Somatic; CYP11B1, Cytochrome P450 Family 1 Subfamily B Member 1; DCT, Dopachrome Tautomerase; DDB2, Damage Specific DNA Binding Protein 2; DEFB4A, Defensin Beta 4A; DNMT1, DNA Methyltransferase 1; EGF, Epidermal Growth Factor; ELANE, Elastase, Neutrophil Expressed; ELN, Elastin; ESR1, Estrogen Receptor 1; ESR2, Estrogen Receptor 2; EZH2, Enhancer Of Zeste 2 Polycomb Repressive Complex 2 Subunit; F2RL1, F2R Like Trypsin Receptor 1; FASN, Fatty Acid Synthase; FBLN2, Fibulin 2; FBN1, Fibrillin 1; FBN2, Fibrillin 2; FBXO40, F-Box Protein 40; FLG, Filaggrin; FN1, Fibronectin 1; FOSB, FosB Proto-Oncogene; AP-1 Transcription Factor Subunit; GAL, Galanin And GMAP Prepropeptide; GDA, Guanine Deaminase; GNAQ, G Protein Subunit Alpha Q; GPX4, Glutathione Peroxidase 4; GSR, Glutathione-Sulfide Reductase; GZMB, Granzyme B; HBEGF, Heparin Binding EGF Like Growth Factor; HDAC3, Histone Deacetylase 3; HIF1A, Hypoxia Inducible Factor 1 Subunit Alpha; HMMR, Hyaluronan Mediated Motility Receptor; HRH1, Histamine Receptor H1; HSD11B1, Hydroxysteroid 11-Beta Dehydrogenase 1; HSD17B2, Hydroxysteroid 11-Beta Dehydrogenase 2; SD17B4, Hydroxysteroid 11-Beta Dehydrogenase 4; HSD17B8, Hydroxysteroid 11-Beta Dehydrogenase 8; HSPA1A, Heat Shock Protein Family A (Hsp70) Member 1A; HSPA4, Heat Shock Protein Family A (Hsp70) Member 4; HYAL2, Hyaluronidase 2; IL18R1, Interleukin 18 Receptor 1; IL1A, Interleukin 1 Alpha; IL1B, Interleukin 1 Beta; IL1R1, Interleukin 1 Receptor Type 1; IL6, Interleukin 6; IRAK1, Interleukin 1 Receptor Associated Kinase 1; ITGB1, Integrin Subunit Beta 1; IVL, Involucrin; JUN, Jun proto-oncogene, AP-1 Transcription Factor Subunit; KRT10, Keratin 10; KRT14, Keratin 14; KRT16, Keratin 16; KRT19, Keratin 19; LMNA, Lamin A/C; LMNB1, LOX, Lysyl Oxidase, MAPK1, Mitogen-Activated Protein Kinase 1; MAPK3, Mitogen-Activated Protein Kinase 3; MAPK10, Mitogen-Activated Protein Kinase 10; MAPK14, Mitogen-Activated Protein Kinase 14; MDM2, MDM2 Proto-Oncogene; MFAP2, Microfibril Associated Protein 2; MITF, Melanocyte Inducing Transcription Factor; MMP1, Matrix Metalloproteinase 1; MMP2, Matrix Metalloproteinase 2; MMP3, Matrix Metalloproteinase 3; MMP7, Matrix Metalloproteinase 7; MMP8, Matrix Metalloproteinase 8; MMP9, Matrix Metalloproteinase 9; MMP10, Matrix Metalloproteinase 10; MMP13, Matrix Metalloproteinase 13; MMP14, Matrix Metalloproteinase 14; MTOR, Mechanistic Target Of Rapamycin Kinase; MYC, MYC Proto-Oncogene, BHLH Transcription Factor; MYD88, MYD88 Innate Immune Signal Transduction Adaptor; NFE2L2, NFE2 Like BZIP Transcription Factor 2; NFKB1, Nuclear Factor Kappa B Subunit 1; NFKBIA, NFKB Inhibitor Alpha; NOS2, Nitric Oxide Synthase 2; NR1H2, Nuclear Receptor Subfamily 1 Group H Member 2; NR1H3, Nuclear Receptor Subfamily 1 Group H Member 3; ODC1, Ornithine Decarboxylase 1; OPN1SW, Opsin 1, Short Wave Sensitive; OPN3, Opsin 3; OPN4, Opsin 4; ORAI1, ORAI Calcium Release-Activated Calcium Modulator 1; PDYN, Prodynorphin; PEX7, Peroxisomal Biogenesis Factor 7; PIK3CG, Phosphatidylinositol-4,5-Bisphosphate 3-Kinase Catalytic Subunit Gamma; PIK3R1, Phosphoinositide-3-Kinase Regulatory Subunit 1; PLA2G4A, Phospholipase A2 Group IVA; POSTN, Periostin; PPARD, Peroxisome Proliferator Activated Receptor delta; PPARG, Peroxisome Proliferator Activated Receptor Gamma; PRF1, Perforin 1; PRKAA2, Protein Kinase AMP-Activated Catalytic Subunit Alpha 2; PRKCD, Protein Kinase C Delta; PSMC4, Proteasome 26S Subunit, ATPase 4; PTEN, Phosphatase And Tensin Homolog; PTGS2, prostaglandin-endoperoxide synthase 2; PTK2, Protein Tyrosine Kinase 2, PTPRK, Protein Tyrosine Phosphatase Receptor Type K; RARA, Retinoic Acid Receptor Alpha; RARB, Retinoic Acid Receptor Beta; RARG, Retinoic Acid Receptor Gamma; RBP1, Retinol Binding Protein 1; RHO, Rhodopsin; RPS27A, Ribosomal Protein S27a; RPS3, Ribosomal Protein S3; RXRB, Retinoid X Receptor Beta; S100A8, S100 Calcium Binding Protein A8; SAA1, Serum Amyloid A1; SCD, Stearoyl-CoA Desaturase; SERPINH1, Serpin Family H Member 1; SFN, Stratifin; SIRT1, Sirtuin 1; SMAD2, SMAD Family Member 2; SMAD4, SMAD Family Member 4; SMAD7, SMAD Family Member 7; SOD1, Superoxide Dismutase 1; SOD2, Superoxide Dismutase 2; SPARC, Secreted Protein Acidic And Cysteine Rich; SPRR1B, Small Proline Rich Protein 1B; STK11, Serine/Threonine Kinase 11; SULT1E1, Sulfotransferase Family 1E Member 1; TCF7L2, Transcription Factor 7 Like 2; TEP1, Telomerase Associated Protein 1; TGFB1, Transforming Growth Factor Beta 1; TGFB3, Transforming Growth Factor Beta 3; TGFB2, Transforming Growth Factor Beta Receptor 2; TGM1, Transglutaminase 1; TIMP1, Tissue Inhibitor of the Metalloproteinases 1; TLR4, Toll-Like Receptor 4; TNF, Tumor Necrosis Factor; TP53, Tumor Protein P53; TYR, Tyrosinase; TYRP1, Tyrosinase Related Protein 1; VEGFA, Vascular Endothelial Growth Factor A; XAB2, XPA Binding Protein 2; XDH, Xanthine Dehydrogenase; XPA, DNA Damage Recognition And Repair Factor.

almost alter UVA-induced gene expression of TGF- β 1, TGF- β 3, TIMP1, SMAD4 and SMAD7 to the normal level (Fig. 4). This demonstrated the reliability of the joint effect of network pharmacology and *in vitro* experiments. Moreover, asiaticoside was previously shown to suppress TGF- β /Smad signalling through inducing Smad7 and PPAR γ in fibroblasts,¹⁵ which further confirmed our conjecture that asiaticoside could inhibit UVA-induced photodamage by activating the TGF- β /Smad pathway. HDFs exposed to UVA released a range of inflammation factors including IL-6 and TNF- α , the critical trigger for cell apoptosis and skin aging.⁴⁹ IL-6 and TNF- α were significantly enriched in the NF- κ B signalling pathway (Fig. 2, Table S2), which were the downstream signalling factors and essential activators for the NF- κ B pathway.³⁴ The raised gene expression of IL-6 and TNF- α in UVA-exposed HDFs indicated the activation of the NF- κ B pathway. But this phenomenon can be reversed by 25 μ g/mL asiaticoside treatment (Fig. 4). Suppressed PI3K-AKT signalling pathway was found in photoaged HDFs, which could accelerate cell apoptosis.⁴ PTEN and PPAR γ

are known significant negative regulators of PI3K-AKT signalling by decreasing the expression of p-AKT⁴ and PIK3R1 contributed to the PI3K activity.³⁵ Anti-apoptotic BCL2L1 could directly activate PI3K-AKT pathway,⁵⁰ with pro-apoptotic BAX and P53 stimulating an opposite effect.⁵¹ As reported, BCL2L1 and BAX are also the downstream targets of the NF- κ B pathway,^{52,53} which could inhibit NF- κ B activity and abrogate p53-induced apoptosis.⁵⁴ This indicated that the NF- κ B pathway was closely related to the PI3K-AKT pathway in the photoaging progression. Moreover, TGF- β can activate the PI3K-AKT pathway.⁵⁵ MAPK could exert a synergistic effect on PI3K-AKT pathway⁵⁶ and disrupt NF- κ B dependent inflammatory stress.⁵⁷ Longevity regulating pathway played antagonistic roles in response to the NF- κ B pathway.⁵⁸ Such evidence gives us a hint that PI3K-AKT and NF- κ B signalling pathways may play a central role in asiaticoside-induced photoaging alleviation. Compared to the control group, exposure to UVA radiation significantly increased the expression of PTEN, PPAR γ , BAX, and P53 while decreasing the expression of PIK3R1 and BCL2L1 as shown

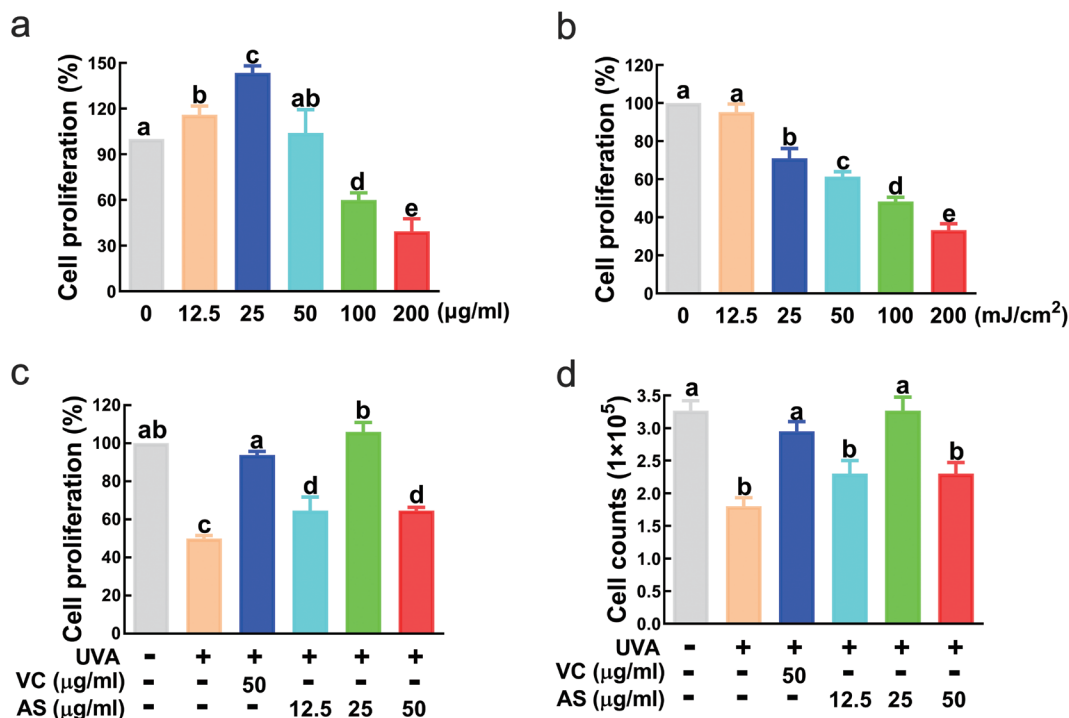


Fig. 3. UVA-induced photoaging of HDFs and asiaticoside rescued the effect. (a) Effect of varying asiaticoside concentrations on HDFs proliferation at 48 h post-treatment. (b) Effect of different UVA doses with different doses on HDFs proliferation at 48 h post-irradiation. The influence of asiaticoside on the proliferation of UVA-irradiated HDFs using the CCK-8 assay (c) and manual cell counting (d) after 48 h treatment. Each experiment was conducted with at least 3 independent cell samples. Different lowercase letters indicate significant differences between the specified groups ($p < 0.05$). AS, asiaticoside; CCK-8, cell counting kit 8; HDFs, human dermal fibroblasts; UVA, ultraviolet A; VC, vitamin C.

in Figure 4a ($p < 0.05$). However, 25 µg/mL asiaticoside treatment could significantly rescue UVA-induced those gene expressions (Fig. 4a, $p < 0.05$). WB assay also implicated the activation of the NF-κB pathway and suppression of PI3K-AKT in UVA-irradiated HDFs, but this effect could be regressed by 25 µg/mL asiaticoside treatments (Fig. 4b).

The molecular docking analysis revealed that asiaticoside exhibited a high binding affinity with the co-core proteins (Fig. 5). The findings suggest that asiaticoside may play a significant role in the treatment of photoaging by targeting the core proteins and related pathways.

Future directions

The study provided a thorough and systematic insight into the possible therapeutic mechanism of asiaticoside for the treatment of photoaging. Future research will be conducted to support this theory, including further confirmation by *in vitro* and *in vivo* investigations.

Conclusion

Achieving the objectives of preventing skin photoaging and improving the appearance of fine, as well as, coarse wrinkles is a crucial aim of skincare treatments. Currently, available anti-photoaging agents often target a single aspect, such as antioxidants. However, a drug that can target multiple aspects of the photoaging mechanism with minimal side effects would be a preferred therapeutic agent. Asiaticoside is a promising multi-targeting drug that has shown potential in photoprotection. It has been shown to reverse the in-

hibition of HDF proliferation caused by UVA irradiation, including the modulation of the expression levels of genes related to collagen degradation, inflammation, and apoptosis in UVA-irradiated HDFs. Further mechanistic studies have demonstrated that asiaticoside exerts its multi-targeting effect mainly by activating the PI3K-AKT pathway and inhibiting the NF-κB pathway, which triggers a series of anti-photoaging cascades. The findings suggest that asiaticoside could be an attractive anti-photoaging agent in the future.

Supporting information

Supplementary material for this article is available at <https://doi.org/10.14218/ERHM.2023.00037>.

Table S1. Target prediction result for asiaticoside.

Table S2. KEGG enrichment analysis of core genes by Metascape.

Acknowledgments

None to declare.

Funding

The study was supported by the fundamental research program funding of Ninth People’s Hospital affiliated with Shanghai Jiao Tong University School of Medicine (JYZZ176) and the National Natural Science Foundation of China (grant no. 82104485)

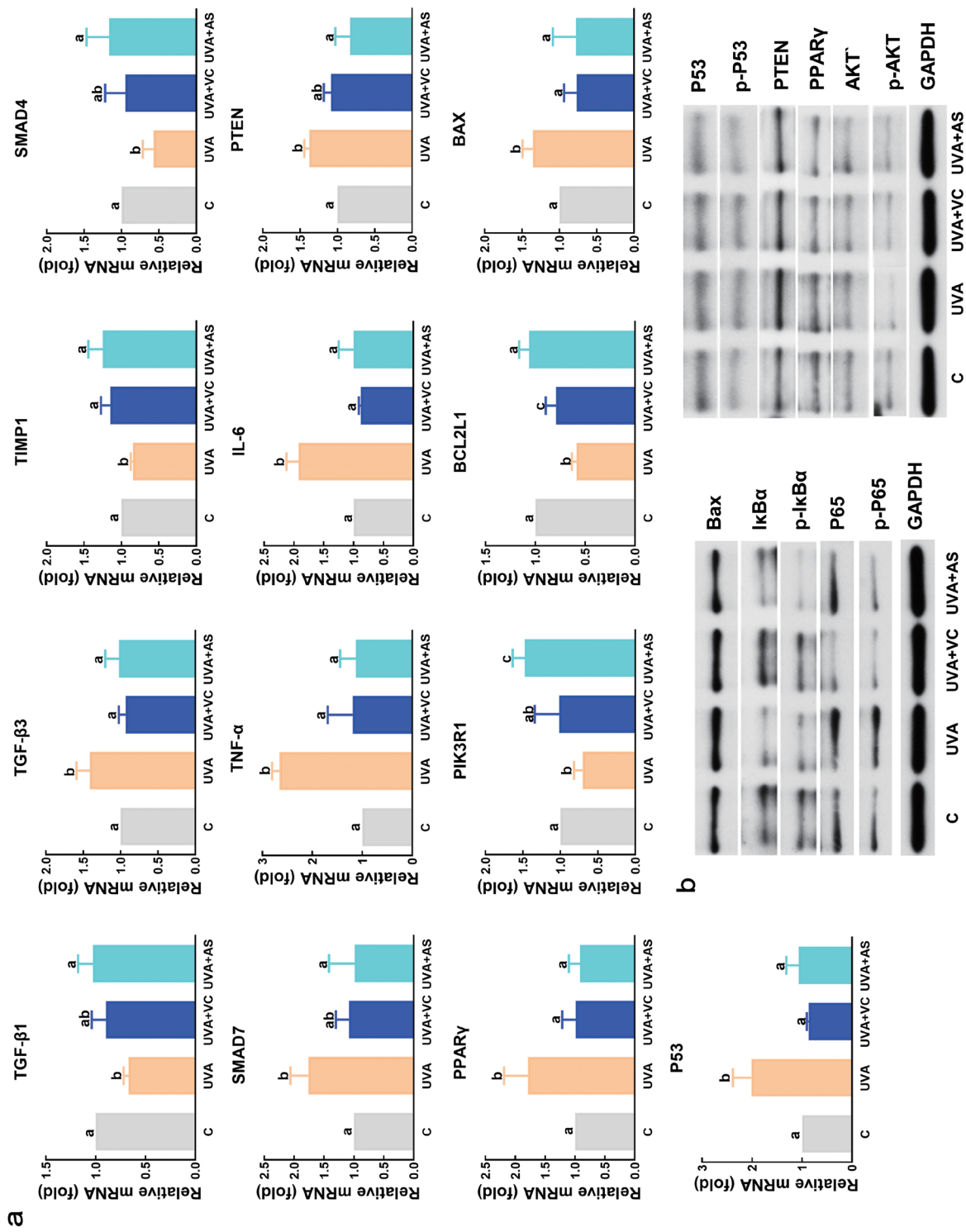


Fig. 4. Asiaticoside reversed UVA-induced expression levels of genes and proteins related to photoaging mined by network pharmacology. (a) Asiaticoside reversed UVA-altered gene expression with significant differences as indicated. (b) Asiaticoside reversed UVA-altered protein expression. C, UVA, UVA+VC, UVA+AS represented the non-irradiated, UVA-irradiated, UVA and vitamin C treated, UVA and 25 μ g/mL asiaticoside treated groups, respectively. The experiments were carried out on at least 3 separate cell samples for each assay. Different lowercase letters represent significant differences among indicated groups ($p < 0.05$). AKT, protein kinase B; AS, asiaticoside; BAX, BCL2-like 1; BCL2L1, BCL2 like 1 (human); IL6, Interleukin 6; P53, tumor protein p53; p-AKT, phospho-AKT; PIK3R1, phosphoinositide-3-kinase regulatory subunit 1; PPAR- γ , Peroxisome Proliferator Activated Receptor gamma; PTEN, Phosphatase And Tensin Homolog; SMAD4, suppressor of mothers against decapentaplegic 4; TNF- α , tumour necrosis factor- α ; UVA, ultraviolet A; VC, vitamin C.

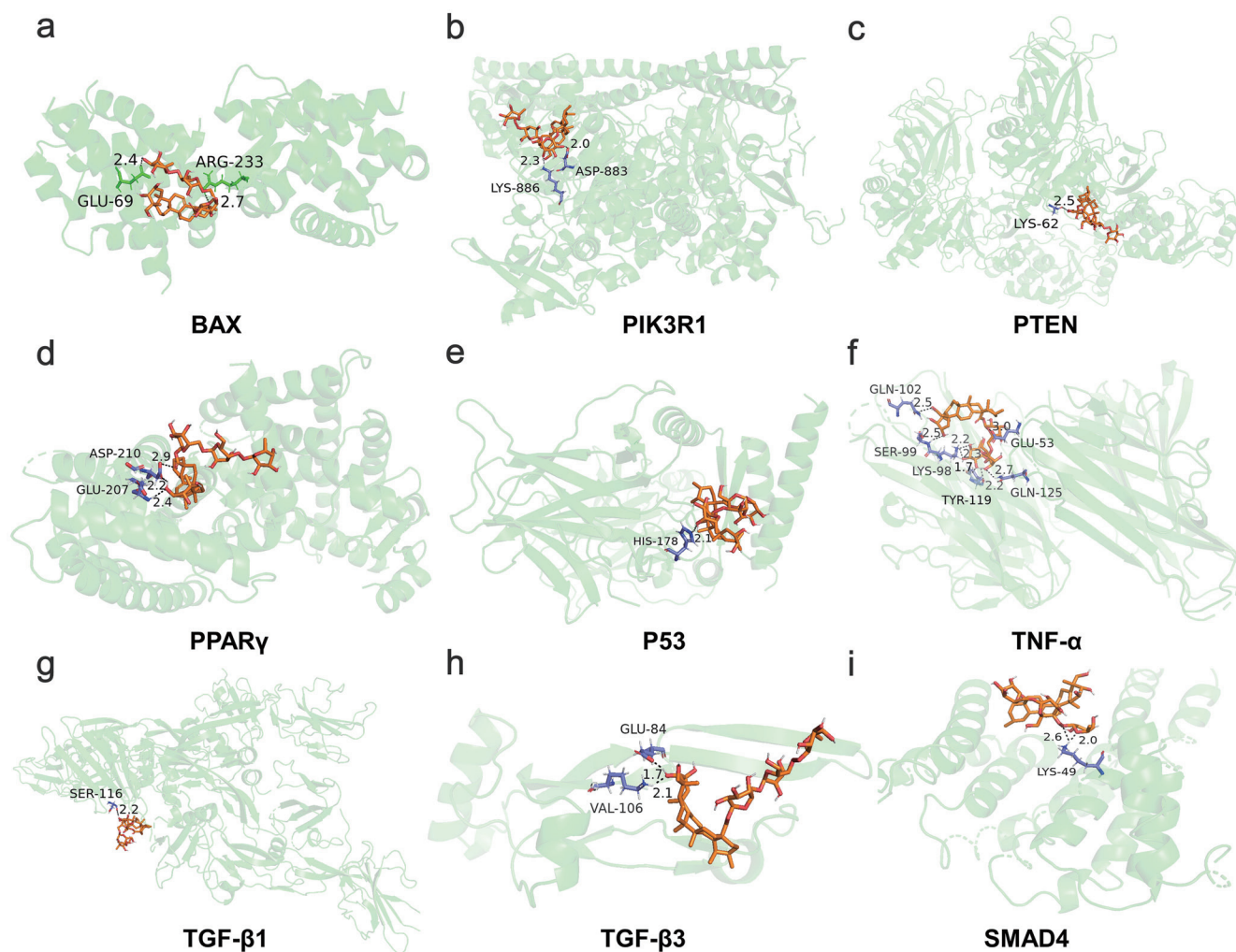


Fig. 5. Molecular docking of asiaticoside and core proteins. Molecular docking results of asiaticoside with BAX (a), PIK3R1 (b), PTEN (c), PPAR γ (d), P53 (e), TNF- α (f), TGF- β 1 (g), TGF- β 3 (h), SMAD4 (i) protein with asiaticoside. BAX, BCL-2-associated X protein; PIK3R1, phosphoinositide-3-kinase regulatory subunit 1; PPAR γ , peroxisome proliferator-activated receptor gamma; PTEN, phosphatase and tensin homolog; SMAD, suppressor of mothers against decapentaplegic; TGF β , transforming growth factor-beta; TNF- α , tumour necrosis factor- α .

Conflict of interest

The authors have declared no conflict of interests.

Author contributions

Data curation, formal analysis, visualization and writing-original draft (JH); Investigation and Software (YYG and KL); Supervision (JC and XBZ); Conceptualization, writing-review & editing (XBZ).

Data sharing statement

No additional data are available.

Ethical statement

All procedures performed in this study involving human participants, were in accordance with the ethical standards of the Fudan

University School of Medicine (Ethical approval document No: 2022-778) and with the 1964 Helsinki declaration and its later amendments. Written and informed consent for publication was obtained from male donors.

References

- [1] Van Pham P, Dang LT, Dinh UT, Truong HT, Huynh BN, Van Le D, *et al*. In vitro evaluation of the effects of human umbilical cord extracts on human fibroblasts, keratinocytes, and melanocytes. *In Vitro Cell Dev Biol Anim* 2014;50(4):321–330. doi:10.1007/s11626-013-9706-1, PMID:24163162.
- [2] Li Y, Zeng N, Qin Z, Chen Y, Lu Q, Cheng Y, *et al*. Ultrasmall Prussian blue nanoparticles attenuate UVA-induced cellular senescence in human dermal fibroblasts via inhibiting the ERK/AP-1 pathway. *Nanoscale* 2021;13(38):16104–16112. doi:10.1039/d1nr04268h, PMID:34486632.
- [3] Morgan MJ, Liu ZG. Crosstalk of reactive oxygen species and NF- κ B signaling. *Cell Res* 2011;21(1):103–115. doi:10.1038/cr.2010.178, PMID:21187859.

- [4] Chen K, Zhu P, Chen W, Luo K, Shi XJ, Zhai W. Melatonin inhibits proliferation, migration, and invasion by inducing ROS-mediated apoptosis via suppression of the PI3K/Akt/mTOR signaling pathway in gallbladder cancer cells. *Aging (Albany NY)* 2021;13(18):22502–22515. doi:10.18632/aging.203561, PMID:34580235.
- [5] Wu Y, Wang J, Zhao T, Wei Y, Han L, Shen L, *et al*. LncRNAs activate longevity regulation pathway due to aging of Leydig cells caused by DEHP exposure: A transcriptome-based study. *Ecotoxicol Environ Saf* 2021; 209:111798. doi:10.1016/j.ecoenv.2020.111798, PMID:33360214.
- [6] Oh JH, Kim J, Karadeniz F, Kim HR, Park SY, Seo Y, *et al*. Santamarine Shows Anti-Photoaging Properties via Inhibition of MAPK/AP-1 and Stimulation of TGF- β /Smad Signaling in UVA-Irradiated HDFs. *Molecules* 2021;26(12):3585. doi:10.3390/molecules26123585, PMID:34208202.
- [7] Park MY, Sohn S, Lee ES, Kim YC. Photorejuvenation induced by 5-aminolevulinic acid photodynamic therapy in patients with actinic keratosis: a histologic analysis. *J Am Acad Dermatol* 2010;62(1):85–95. doi:10.1016/j.jaad.2009.06.025, PMID:19926165.
- [8] Li XM, Peng JH, Sun ZL, Tian HJ, Duan XH, Liu L, *et al*. Chinese medicine CGA formula ameliorates DMN-induced liver fibrosis in rats via inhibiting MMP2/9, TIMP1/2 and the TGF- β /Smad signaling pathways. *Acta Pharmacol Sin* 2016;37(6):783–793. doi:10.1038/aps.2016.35, PMID:27133300.
- [9] An L, Li Z, Shi L, Wang L, Wang Y, Jin L, *et al*. Inflammation-Targeted Celastrol Nanodrug Attenuates Collagen-Induced Arthritis through NF- κ B and Notch1 Pathways. *Nano Lett* 2020;20(10):7728–7736. doi:10.1021/acs.nanolett.0c03279, PMID:32965124.
- [10] Hwang JY, Yadav AK, Jang BC, Kim YC. Antioxidant and cytoprotective effects of *Stachys riederi* var. *japonica* ethanol extract on UVA-irradiated human dermal fibroblasts. *Int J Mol Med* 2019;43(3):1497–1504. doi:10.3892/ijmm.2019.4048, PMID:30628642.
- [11] Oh JH, Joo YH, Karadeniz F, Ko J, Kong CS. Syringaresinol Inhibits UVA-Induced MMP-1 Expression by Suppression of MAPK/AP-1 Signaling in HaCaT Keratinocytes and Human Dermal Fibroblasts. *Int J Mol Sci* 2020;21(11):3981. doi:10.3390/ijms21113981, PMID:32492931.
- [12] Myung DB, Lee JH, Han HS, Lee KY, Ahn HS, Shin YK, *et al*. Oral Intake of *Hydrangea serrata* (Thunb.) Ser. Leaves Extract Improves Wrinkles, Hydration, Elasticity, Texture, and Roughness in Human Skin: A Randomized, Double-Blind, Placebo-Controlled Study. *Nutrients* 2020;12(6):1588. doi:10.3390/nu12061588, PMID:32481760.
- [13] Zussman J, Ahdout J, Kim J. Vitamins and photoaging: do scientific data support their use? *J Am Acad Dermatol* 2010;63(3):507–525. doi:10.1016/j.jaad.2009.07.037, PMID:20189681.
- [14] Namviriyachote N, Muangman P, Chinaroonchai K, Chuntrasakul C, Ritthidej GC. Polyurethane-biomacromolecule combined foam dressing containing asiaticoside: fabrication, characterization and clinical efficacy for traumatic dermal wound treatment. *Int J Biol Macromol* 2020;143:510–520. doi:10.1016/j.ijbiomac.2019.10.166, PMID:31778697.
- [15] Huang J, Zhou X, Xia L, Liu W, Guo F, Liu J, *et al*. Inhibition of hypertrophic scar formation with oral asiaticoside treatment in a rabbit ear scar model. *Int Wound J* 2021;18(5):598–607. doi:10.1111/iwj.13561, PMID:33666348.
- [16] Arora R, Kumar R, Agarwal A, Reeta KH, Gupta YK. Comparison of three different extracts of *Centella asiatica* for anti-amnesic, antioxidant and anticholinergic activities: in vitro and in vivo study. *Biomed Pharmacother* 2018;105:1344–1352. doi:10.1016/j.biopha.2018.05.156, PMID:30021372.
- [17] Wan J, Gong X, Jiang R, Zhang Z, Zhang L. Antipyretic and anti-inflammatory effects of asiaticoside in lipopolysaccharide-treated rat through up-regulation of heme oxygenase-1. *Phytother Res* 2013;27(8):1136–1142. doi:10.1002/ptr.4838, PMID:22972613.
- [18] Yuan H, Ma Q, Cui H, Liu G, Zhao X, Li W, *et al*. How Can Synergism of Traditional Medicines Benefit from Network Pharmacology? *Molecules* 2017;22(7):1135. doi:10.3390/molecules22071135, PMID:28686181.
- [19] Jameel M, Jamal K, Alam MF, Ameen F, Younus H, Siddique HR. Interaction of thiamethoxam with DNA: Hazardous effect on biochemical and biological parameters of the exposed organism. *Chemosphere* 2020;254:126875. doi:10.1016/j.chemosphere.2020.126875, PMID:32361544.
- [20] Li J, Luo H, Liu X, Zhang J, Zhou W, Guo S, *et al*. Dissecting the mechanism of Yuzhi Zhixue granule on ovulatory dysfunctional uterine bleeding by network pharmacology and molecular docking. *Chin Med* 2020;15:113. doi:10.1186/s13020-020-00392-0, PMID:33110441.
- [21] Gong R, Ren S, Chen M, Wang Y, Zhang G, Shi L, *et al*. Bioinformatics Analysis Reveals the Altered Gene Expression of Patients with Postmenopausal Osteoporosis Using Liuweidihuang Pills Treatment. *Biomed Res Int* 2019;2019:1907906. doi:10.1155/2019/1907906, PMID:30809532.
- [22] Daina A, Michielin O, Zoete V. SwissTargetPrediction: updated data and new features for efficient prediction of protein targets of small molecules. *Nucleic Acids Res* 2019;47(W1):W357–W364. doi:10.1093/nar/gkz382, PMID:31106366.
- [23] Wang X, Shen Y, Wang S, Li S, Zhang W, Liu X, *et al*. PharmMapper 2017 update: a web server for potential drug target identification with a comprehensive target pharmacophore database. *Nucleic Acids Res* 2017;45(W1):W356–W360. doi:10.1093/nar/gkx374, PMID:28472422.
- [24] Grondin CJ, Davis AP, Wiegers JA, Wiegers TC, Sciaky D, Johnson RJ, *et al*. Predicting molecular mechanisms, pathways, and health outcomes induced by Juul e-cigarette aerosol chemicals using the Comparative Toxicogenomics Database. *Curr Res Toxicol* 2021;2:272–281. doi:10.1016/j.crtox.2021.08.001, PMID:34458863.
- [25] Paolacci S, Precone V, Acquaviva F, Chiurazzi P, Fulcheri E, Pinelli M, *et al*. Genetics of lipedema: new perspectives on genetic research and molecular diagnoses. *Eur Rev Med Pharmacol Sci* 2019;23(13):5581–5594. doi:10.26355/eurrev_201907_18292, PMID:31298310.
- [26] Reimand J, Isserlin R, Voisin V, Kucera M, Tannus-Lopes C, Rostamianfar A, *et al*. Pathway enrichment analysis and visualization of omics data using g:Profiler, GSEA, Cytoscape and EnrichmentMap. *Nat Protoc* 2019;14(2):482–517. doi:10.1038/s41596-018-0103-9, PMID:30664679.
- [27] Lu X, Yu S, Lü P, Chen H, Zhong S, Zhou B. Genome-Wide Transcriptomic Analysis Reveals a Regulatory Network of Oxidative Stress-Induced Flowering Signals Produced in Litchi Leaves. *Genes (Basel)* 2020;11(3):324. doi:10.3390/genes11030324, PMID:32197528.
- [28] Zhang H, Fu Q, Shi X, Pan Z, Yang W, Huang Z, *et al*. Human A-to-I RNA editing SNP loci are enriched in GWAS signals for autoimmune diseases and under balancing selection. *Genome Biol* 2020;21(1):288. doi:10.1186/s13059-020-02205-x, PMID:33256812.
- [29] Huang B, Han W, Sheng ZF, Shen GL. Identification of immune-related biomarkers associated with tumorigenesis and prognosis in cutaneous melanoma patients. *Cancer Cell Int* 2020;20:195. doi:10.1186/s12935-020-01271-2, PMID:32508531.
- [30] Huang J, Zhou X, Shen Y, Li H, Zhou G, Zhang W, *et al*. Asiaticoside loading into polylactic-co-glycolic acid electrospun nanofibers attenuates host inflammatory response and promotes M2 macrophage polarization. *J Biomed Mater Res A* 2020;108(1):69–80. doi:10.1002/jbm.a.36793, PMID:31496042.
- [31] Tominaga K, Suzuki HI. TGF- β Signaling in Cellular Senescence and Aging-Related Pathology. *Int J Mol Sci* 2019;20(20):5002. doi:10.3390/ijms20205002, PMID:31658594.
- [32] Wan SZ, Liu C, Huang CK, Luo FY, Zhu X. Ursolic Acid Improves Intestinal Damage and Bacterial Dysbiosis in Liver Fibrosis Mice. *Front Pharmacol* 2019;10:1321. doi:10.3389/fphar.2019.01321, PMID:31736766.
- [33] Liu Z, Li Y, Song H, He J, Li G, Zheng Y, *et al*. Collagen peptides promote photoaging skin cell repair by activating the TGF- β /Smad pathway and depressing collagen degradation. *Food Funct* 2019;10(9):6121–6134. doi:10.1039/c9fo00610a, PMID:31497829.
- [34] Fujita K, Tokuda H, Yamamoto N, Kainuma S, Kawabata T, Sakai G, *et al*. Incretins amplify TNF- α -stimulated IL-6 synthesis in osteoblasts: Suppression of the I κ B/NF- κ B pathway. *Int J Mol Med* 2017;39(4):1053–1060. doi:10.3892/ijmm.2017.2892, PMID:28204823.
- [35] Kawaguchi A, Yajima N, Komohara Y, Aoki H, Tsuchiya N, Homma J, *et al*. Identification and validation of a gene expression signature that predicts outcome in malignant glioma patients. *Int J Oncol* 2012;40(3):721–730. doi:10.3892/ijo.2011.1240, PMID:22021018.
- [36] Duan S, Yu S, Yuan T, Yao S, Zhang L. Exogenous Let-7a-5p Induces A549 Lung Cancer Cell Death Through BCL2L1-Mediated PI3Ky Signaling Pathway. *Front Oncol* 2019;9:808. doi:10.3389/fonc.2019.00808,

- PMID:31508368.
- [37] Li Q, Wang X, Wu X, Rui Y, Liu W, Wang J, *et al*. Daxx cooperates with the Axin/HIPK2/p53 complex to induce cell death. *Cancer Res* 2007;67(1):66–74. doi:10.1158/0008-5472.CAN-06-1671, PMID:17210684.
- [38] Liu Y, Hwang E, Ngo HTT, Perumalsamy H, Kim YJ, Li L, *et al*. Protective Effects of Euphrasia officinalis Extract against Ultraviolet B-Induced Photoaging in Normal Human Dermal Fibroblasts. *Int J Mol Sci* 2018;19(11):3327. doi:10.3390/ijms19113327, PMID:30366440.
- [39] Kim HR, Kim S, Lee SW, Sin HS, Kim SY. Protective Effects of Fermented Paprika (*Capsicum annuum* L.) on Sodium Iodate-Induced Retinal Damage. *Nutrients* 2020;13(1):25. doi:10.3390/nu13010025, PMID:33374795.
- [40] Lee S, Hoang GD, Kim D, Song HS, Choi S, Lee D, *et al*. Efficacy of Alpinumisoflavone Isolated from *Maclura tricuspidata* Fruit in Tumor Necrosis Factor- α -Induced Damage of Human Dermal Fibroblasts. *Antioxidants (Basel)* 2021;10(4):514. doi:10.3390/antiox10040514, PMID:33806207.
- [41] Kim KH, Park SJ, Lee JY, Lee JE, Song CH, Choi SH, *et al*. Inhibition of UVB-induced skin damage by exopolymers from *Aureobasidium pullulans* SM-2001 in hairless mice. *Basic Clin Pharmacol Toxicol* 2015;116(2):73–86. doi:10.1111/bcpt.12288, PMID:24964914.
- [42] Mimeault M, Batra SK. Recent insights into the molecular mechanisms involved in aging and the malignant transformation of adult stem/progenitor cells and their therapeutic implications. *Ageing Res Rev* 2009;8(2):94–112. doi:10.1016/j.arr.2008.12.001, PMID:19114129.
- [43] Ingram DK, Zhu M, Mamczarz J, Zou S, Lane MA, Roth GS, *et al*. Calorie restriction mimetics: an emerging research field. *Ageing Cell* 2006;5(2):97–108. doi:10.1111/j.1474-9726.2006.00202.x, PMID:16626389.
- [44] Lee YR, Noh EM, Kwon KB, Lee YS, Chu JP, Kim EJ, *et al*. *Radix clematidis* extract inhibits UVB-induced MMP expression by suppressing the NF- κ B pathway in human dermal fibroblasts. *Int J Mol Med* 2009;23(5):679–684. doi:10.3892/ijmm_00000180, PMID:19360328.
- [45] Zhang JA, Yin Z, Ma LW, Yin ZQ, Hu YY, Xu Y, *et al*. The protective effect of baicalin against UVB irradiation induced photoaging: an in vitro and in vivo study. *PLoS One* 2014;9(6):e99703. doi:10.1371/journal.pone.0099703, PMID:24949843.
- [46] Jeon H, Kim DH, Nho YH, Park JE, Kim SN, Choi EH. A Mixture of Extracts of *Kochia scoparia* and *Rosa multiflora* with PPAR α/γ Dual Agonistic Effects Prevents Photoaging in Hairless Mice. *Int J Mol Sci* 2016;17(11):1919. doi:10.3390/ijms17111919, PMID:27854351.
- [47] Zhang M, Qureshi AA, Geller AC, Frazier L, Hunter DJ, Han J. Use of tanning beds and incidence of skin cancer. *J Clin Oncol* 2012;30(14):1588–1593. doi:10.1200/JCO.2011.39.3652, PMID:22370316.
- [48] Pantke S, Fricke TC, Eberhardt MJ, Herzog C, Leffler A. Gating of the capsaicin receptor TRPV1 by UVA-light and oxidants are mediated by distinct mechanisms. *Cell Calcium* 2021;96:102391. doi:10.1016/j.ceca.2021.102391, PMID:33752082.
- [49] Xia S, Zhang X, Zheng S, Khanabdali R, Kalionis B, Wu J, *et al*. An Update on Inflamm-Aging: Mechanisms, Prevention, and Treatment. *J Immunol Res* 2016;2016:8426874. doi:10.1155/2016/8426874, PMID:27493973.
- [50] Ramezani-Rad P, Geng H, Hurtz C, Chan LN, Chen Z, Jumaa H, *et al*. SOX4 enables oncogenic survival signals in acute lymphoblastic leukemia. *Blood* 2013;121(1):148–155. doi:10.1182/blood-2012-05-428938, PMID:23152540.
- [51] Sadidi M, Lentz SI, Feldman EL. Hydrogen peroxide-induced Akt phosphorylation regulates Bax activation. *Biochimie* 2009;91(5):577–585. doi:10.1016/j.biochi.2009.01.010, PMID:19278624.
- [52] Zhang B, Chu S, Agarwal P, Campbell VL, Hopcroft L, Jørgensen HG, *et al*. Inhibition of interleukin-1 signaling enhances elimination of tyrosine kinase inhibitor-treated CML stem cells. *Blood* 2016;128(23):2671–2682. doi:10.1182/blood-2015-11-679928, PMID:27621307.
- [53] Lin Y, Bai L, Chen W, Xu S. The NF- κ B activation pathways, emerging molecular targets for cancer prevention and therapy. *Expert Opin Ther Targets* 2010;14(1):45–55. doi:10.1517/14728220903431069, PMID:20001209.
- [54] Xiao X, Yang G, Bai P, Gui S, Nyuyen TM, Mercado-Urbe I, *et al*. Inhibition of nuclear factor- κ B enhances the tumor growth of ovarian cancer cell line derived from a low-grade papillary serous carcinoma in p53-independent pathway. *BMC Cancer* 2016;16:582. doi:10.1186/s12885-016-2617-2, PMID:27484466.
- [55] Ottley E, Gold E. microRNA and non-canonical TGF- β signalling: implications for prostate cancer therapy. *Crit Rev Oncol Hematol* 2014;92(1):49–60. doi:10.1016/j.critrevonc.2014.05.011, PMID:24985060.
- [56] Forget A, Martignetti L, Puget S, Calzone L, Brabetz S, Picard D, *et al*. Aberrant ERBB4-SRC Signaling as a Hallmark of Group 4 Medulloblastoma Revealed by Integrative Phosphoproteomic Profiling. *Cancer Cell* 2018;34(3):379–395.e7. doi:10.1016/j.ccell.2018.08.002, PMID:30205043.
- [57] Ramalingam P, Poulos MG, Lazzari E, Gutkin MC, Lopez D, Kloss CC, *et al*. Chronic activation of endothelial MAPK disrupts hematopoiesis via NF κ B dependent inflammatory stress reversible by SCGF. *Nat Commun* 2020;11(1):666. doi:10.1038/s41467-020-14478-8, PMID:32015345.
- [58] Zhang WS, Pan A, Zhang X, Ying A, Ma G, Liu BL, *et al*. Inactivation of NF- κ B2 (p52) restrains hepatic glucagon response via preserving PDE4B induction. *Nat Commun* 2019;10(1):4303. doi:10.1038/s41467-019-12351-x, PMID:31541100.